MECHANICS OF STRUCTURED MEDIA

MECHANICS OF STRUCTURED MEDIA

by

Xiaode Niu M.Eng.

A Thesis

Submitted to the School of Graduate Studies

in Partial Fulfilment of the Requirements

for the Degree

Master of Engineering

McMaster University

November 1991

MASTER OF ENGINEERING (1991)
(Civil Engineering
and Engineering Mechanics)

McMASTER UNIVERSITY
Hamilton, Ontario,
Canada

TITLE: Mechanics of Structured Media

AUTHOR: Xiaode Niu

(M.Eng. - Huazhong University of Science
and Technology, China)

SUPERVISOR: Dr. S. Pietruszczak

NUMBER OF PAGES: xi, 99

ABSTRACT

The research reported in this thesis is related to the mathematical description of the response of structured media. Three separate but conceptually linked topics are addressed. Firstly, a mathematical formulation for the description of average mechanical properties of structural masonry is presented. An element of structural masonry is regarded as a composite medium consisting of brick matrix intercepted by the sets of head and bed joints. The former are treated as aligned, uniformly dispersed weak inclusions, whereas the latter as continuous planes of weakness. A general three-dimensional formulation is provided and is subsequently applied to estimate the average elastic properties of masonry and to investigate the conditions at failure.

Subsequently, the approach mentioned above is extended to predict the elastic and elastoplastic properties of fibre and particle reinforced composite systems. An elastic material, with the mechanical properties of the reinforcement, is intercepted by two/three families of mutually orthogonal layers that possess the elastoplastic properties of the matrix. This system is then assumed to be equivalent to a fibre/particle reinforced composite after an appropriate orientation average is evaluated. The predictions of the elastic constants are satisfactory as compared to those derived from the equivalent inclusion method. The simulations of the elastoplastic response of a fibrous composite are also in a qualitative agreement with the experimental observation.

Finally, the finite element method is employed to study the deformation of strain softening materials. Strain softening is considered as the localization of deformation into a shear band, which is treated as a bifurcation problem. A criterion is suggested for the selection of the inclination of a shear band from the multi-solutions produced by the necessary condition of bifurcation. A partitioning scheme is also proposed for the evaluation of a characteristic length related to the finite element implementation of the formulation. The initial stress method is then used to solve a strip footing problem. The numerical study is aimed at investigating the sensitivity of the load-displacement characteristics to the details of discretization.

ACKNOWLEDGEMENTS

The author is deeply grateful to his supervisor Dr. S. Pietruszczak for his guidance, inspiration and encouragement during the course of the work.

The author is also indebted to Dr. D.F.E. Stolle for his helpful discussions and providing the finite element code required for the completion of the research reported in chapter 4.

Finally, the author wishes to express his sincere thanks to his parents and wife for their understanding, support and patience.

TABLE OF CONTENTS

			PAGE
ABSTRACT			iii
ACKNOWLEDGEMENTS			v
LIST OF FIGURES			ix
CHAPTER	1	Introduction	1
	1.1	General remarks	1
	1.2	Objectives and scope of the research	3
CHAPTER	2	A mathematical description of macroscopic behaviour of masonry	5
	2.1	Introduction	5
	2.2	Macroscopic response of structural masonry	7
	2.3	Average elastic properties of structural masonry	12
	2.4	Description of progressive failure of structural masonry	18
	2.5	Conclusions	24

TABLE OF CONTENTS (Cont'd)

			PAGE
CHAPTER 3		Macroscopic description of elastoplastic behaviour of perfectly bonded composites	40
	3.1	Introduction	40
	3.2	Mathematical formulation	41
	3.3	Elastic properties of fibre and particle reinforced composites	47
	3.4	Elastoplastic response of a fibrous composite	50
	3.5	Conclusions	52
	3.6	Appendix: derivation of concentration tensors	53
CHAPTER 4		Finite element analysis of the response of strain softening materials	64
	4.1	Introduction	64
	4.2	Description of localized deformation	66
	4.3	Selection of the inclination of a shear band	72
	4.4	Partitioning scheme for the evaluation of a characteristic length	73

TABLE OF CONTENTS (Cont'd)

			PAGE
	4.5	Finite element analysis of a footing	74
	4.6	Conclusions	76
CHAPTER	5	Conclusions	89
	5.1	General remarks	89
	5.2	Discussions on further studies	91
BIBLIOGRAPHY			93

LIST OF FIGURES

FIGURE		PAGE
2.1	(a) Geometry of a structural masonry panel; (a) medium (1); (c) medium (1) intercepted by bed joints (after Pietruszczak,1991).	26
2.2	Average elastic properties of structural masonry.	27
2.3	Influence of the head joints on the average elastic properties of masonry.	29
2.4	Influence of the head joints on the average elastic properties of masonry.	31
2.5	Failure envelopes for in-plane biaxial compression-tension tests.	33
2.6	Variation of uniaxial compressive (a) and tensile (b) strength with the orientation of bed joints.	35
2.7	Material characteristics corresponding to biaxial compression test ($\beta = 45^0$; stress ratio:5.0)	36
2.8	Failure envelopes for in-plane biaxial compression tests.	38

LIST OF FIGURES (Cont'd)

FIGURE		PAGE
2.9	Influence of head joints on the response under biaxial conditions (a) biaxial compression-tension; (b) biaxial compression.	39
3.1	Elastic constants of a fibrous composite.	57
3.2	Elastic constants of a particle reinforced composite.	59
3.3	Uniaxial tensile stress-strain diagram of 6061 aluminium.	60
3.4	Verification of the averaging scheme; (a) transverse uniaxial tension; (b) longitudinal pure shear.	61
3.5	Uniaxial tensile stress-strain response; (a) numerical prediction; (b) experimental results (after Kenaga et al., 1987).	62
3.6	Tensile strength of a fibrous composite (experimental data from Kenaga et al., 1987).	63
4.1	A sample intercepted by a shear band.	78
4.2	Finite element meshes.	79
4.3	Load-displacement diagrams of the footing corresponding to different type of discretization.	83

LIST OF FIGURES (Cont'd)

FIGURE **PAGE**

4.4 Maps of vertical ((a) and (c)) and horizontal ((b) and (d)) displacement in the vicinity of the footing at the settlement of s=0.24m and s=0.51m. 86

4.5 Softening zone prior to collapse. 88

CHAPTER 1

INTRODUCTION

1.1 GENERAL REMARKS

A structured medium is defined as any multi-phase continuum that retains distinct interfaces among its constituents such that the geometric characteristics and mechanical properties of the constituents remain unaltered. A structured medium can exist either in a natural state (soils, rocks, ice and wood, ect.) or be obtained artificially (concrete, masonry, fibrous composites, ect.). The constituents can be either in the form of physical entities, such as bricks and mortar in masonry, or in the form of imperfections such as microvoids and microcracks.

In order to model the mechanical properties of such materials, two methodologies can be followed. The phenomenogical approach is based on the overall experimental observation of the mechanical response and it ignores the microscopic identities of the constituents. A successful device for describing the inherent and induced anisotropy as well as the irreversibility of deformation is the introduction of internal variables such as damage tensor (Lemaitre, 1985; Krajcinovic and Fonseka, 1981; Leckie and Onat, 1981; Murakami and Ohno, 1981) or fabric tensor (Cowin, 1985; Pietruszczak and Krucinski, 1989), which can be incorporated into the formulation through the framework of thermodynamics (Lemaitre, 1985; Valanis, 1971) or through functional expansion (Krajcinovic and Fonseka, 1981; Murakami and Ohno, 1981; Pietruszczak and Krucinski, 1989). In the microscopic approach, a structured medium is regarded as an assemblage of discrete constituents and the overall mechanical properties are derived from the geometric characteristics and the mechanical properties of the constituents through an appropriate averaging process. The two approaches exhibit their own advantages and disadvantages. The former usually displays relative simplicity but suffers from an impractical demand of a large number of tests required to determine the material constants for varying volume fractions of the constituents. The latter provides more physical insight and requires only the tests for the determination of the material parameters relevant to the mechanical properties of the constituents; however, the quantitative predictions are not always satisfactory due to complexity arising from the interaction between the constituents.

A knowledge of the mechanical behaviour of structured media is of fundamental importance to their proper engineering and scientific applications. In this thesis, three selected topics relevant to civil and mechanical engineering are investigated by employing a unified mathematical framework. Attention is focused on the description of the average mechanical behaviour of the material under consideration, so that the formulations can be easily incorporated into the existing numerical packages for large scale finite element analysis.

1.2 OBJECTIVES AND SCOPE OF THE RESEARCH

Chapter 2 is concerned with a mathematical formulation for the description of average mechanical properties of masonry. A typical element of structural masonry is viewed as a composite medium consisting of the brick matrix intercepted by the sets of head and bed joints. The former are considered as aligned, uniformly dispersed weak inclusions, whereas the latter represent continuous planes of weakness. A general three-dimensional formulation is provided and is subsequently applied to predict the average macroscopic properties in the elastic range and to investigate the conditions at failure. An extensive numerical study is performed.

In chapter 3, a micromechanical approach is proposed to model the elastoplastic behaviour of fibre and particle reinforced composites. The approach is based on the concept of a "superimposed medium". An elastic material, with the mechanical properties of the reinforcement is intercepted by two/three families of mutually orthogonal layers that possess the elastoplastic properties of the matrix. The above system is assumed to be equivalent to a fibre/particle reinforced composite system after an appropriate orientation average is evaluated. Numerical simulations pertaining to the elastic constants of fibre and particle reinforced composites as well as the elastoplastic response of a fibrous composite are provided.

The objective of chapter 4 is to implement the constitutive relation of a strain softening material into the finite element algorithm. The phenomenon of strain softening is regarded as the localization of deformation into a shear band, which is treated as a bifurcation problem. Upon the formation of the shear band, the material becomes a "structured medium" (i.e. the intact material is intercepted by a shear band), so that its mechanical properties can be derived from the framework of mechanics of composite materials. A criterion is proposed for the selection of the orientation of a shear band from the multi-solutions produced by the necessary condition of bifurcation. Thereafter, the initial stress method is used to solve a geotechnical boundary value problem, a strip footing. The numerical results pertaining to the sensitivity of load-displacement characteristics to the details of discretization are provided. The displacement field in the vicinity of the footing at different settlements and the extend of softening zone prior to collapse are also identified.

CHAPTER 2

A MATHEMATICAL DESCRIPTION OF MACROSCOPIC BEHAVIOUR OF MASONRY

2.1 INTRODUCTION

Over the last few decades the research in structural masonry has concentrated mainly on the experimental testing of brickwork. The results of those investigations have provided a valuable information used to establish empirically or semi-empirically based methodologies for the design of masonry structures. There have been only a few isolated attempts to estimate the properties of masonry in a rigorous analytical manner (e.g. Pande et al., 1989). It is quite apparent however, that an adequate description of these properties is essential for the analysis of complex boundary value problems involving masonry structures.

The mechanical response of masonry can be analyzed by employing the finite element technique. By using the physical and the actual geometric properties of brick units and mortar, the numerical solution to a class of selected problems can be obtained

(Ali and Page, 1989; Afshari and Kaldjian, 1989). There are however serious limitations of this approach. Firstly, the actual geometry of the brickwork may result in ill-conditioning of the algebraic system and/or instability of the numerical solution. Secondly, the approach becomes quite impractical in the context of large-scale masonry structures comprising of a very large number of brick units subjected to a three-dimensional state of stress.

This chapter presents an alternative approach for the description of the behaviour of structural masonry. The methodology followed is based on the framework outlined by Pietruszczak (1991). A typical element of brickwork is regarded as a structured/composite medium for which the average macroscopic properties can be uniquely identified. Thus, a representative volume of the "material" considered is assumed to consist of a number of brick units intercepted by two orthogonal families of joints. The chapter is written in the following sequence. First, a general three-dimensional formulation is provided (after Pietruszczak and Niu, 1991). The average constitutive relation is derived by employing the assumption that the head joints represent a set of aligned weak inclusions and the bed joints form continuous planes of weakness. The formulation is then applied to establish the average elastic properties of the system. Later, the phenomenon of a progressive failure of the brickwork is investigated. An extensive numerical study is carried out; the performance of the framework is verified for a series of biaxial compression-tension and compression-compression tests.

2.2 MACROSCOPIC RESPONSE OF STRUCTURAL MASONRY

Consider a typical element of structural masonry, i.e. a brick panel, as shown schematically in Fig.2.1a, subjected to a uniformly distributed load. On the macroscale, the panel can be regarded as a two-phase composite consisting of brick units intercepted by two orthogonal sets of joints filled with mortar. In order to describe the average mechanical properties of the system, it is convenient to address the influence of head (vertical) and bed joints separately, i.e., invoke the concept of a superimposed medium.

Referring to Fig.2.1b, consider first the brick matrix with a family of head joints (so called medium (1)). The head joints can be treated as aligned, uniformly dispersed weak inclusions embodied in the matrix. The average properties of the medium (1) can be represented by a constitutive relation

$$\dot{\sigma}^{(1)} = [D^{(1)}]\dot{\epsilon}^{(1)} \tag{2.1}$$

where $\sigma^{(1)} = \{\sigma_{11}^{(1)}, \sigma_{22}^{(1)}, \sigma_{33}^{(1)}, \sigma_{12}^{(1)}, \sigma_{13}^{(1)}, \sigma_{23}^{(1)}\}^T$ and $\epsilon^{(1)} = \{\epsilon_{11}^{(1)}, \epsilon_{22}^{(1)}, \epsilon_{33}^{(1)}, \gamma_{12}^{(1)}, \gamma_{13}^{(1)}, \gamma_{23}^{(1)}\}^T$ are the volume averages of stress/strain rates in (1). In particular, the homogenized medium (1) can be regarded as an orthotropic elastic-brittle material. In such a case, the components of $[D^{(1)}]$ can be estimated form Eshelby's (1957) solution to an ellipsoidal inclusion problem combined with Mori-Tanaka's (1973) mean-field theory. The explicit relations defining the components of $[D^{(1)}]$ are provided by Zhao and Weng (1990) and are too complex to be cited here.

The entire masonry panel can now be represented by a homogenized medium (1) stratified by a family of bed joints (2), Fig.2.1c. The bed joints run continuously through the panel and form the weakest link in the microstructure of the system. In particular, the bed joints can be regarded as an elastoplastic medium with mechanical properties defined by

$$\dot{\sigma}^{(2)} = [D^{(2)}]\dot{\epsilon}^{(2)} \tag{2.2}$$

Assuming that both constituents (1) and (2) exist simultaneously and are perfectly bonded, the overall stress/strain rate averages $\dot{\sigma}$ and $\dot{\epsilon}$ can be derived from the averaging rule (Hill, 1963)

$$\dot{\epsilon} = \eta_1\dot{\epsilon}^{(1)}+\eta_2\dot{\epsilon}^{(2)} \tag{2.3}$$

$$\dot{\sigma} = \eta_1\dot{\sigma}^{(1)}+\eta_2\dot{\sigma}^{(2)} \tag{2.4}$$

where η's are the volume fractions of both constituents,

$$\eta_1 = \frac{h}{h+t} \quad ; \quad \eta_2 = \frac{t}{h+t} \tag{2.5}$$

and h and t represent the spacing and the thickness of bed joints, respectively.

The assumption of perfect bonding between the constituents and the equilibrium requirements provide additional kinematic and static constraints

$$[\delta^*]\dot{\epsilon}^{(1)} = [\delta^*]\dot{\epsilon}^{(2)} \tag{2.6}$$

$$[\delta]\dot{\sigma}^{(1)} = [\delta]\dot{\sigma}^{(2)} \tag{2.7}$$

where

$$[\delta^*] = \begin{bmatrix} 1 & 0 & 0 & 0 & 0 & 0 \\ 0 & 0 & 1 & 0 & 0 & 0 \\ 0 & 0 & 0 & 0 & 1 & 0 \end{bmatrix} \quad ; \quad [\delta] = \begin{bmatrix} 0 & 1 & 0 & 0 & 0 & 0 \\ 0 & 0 & 0 & 1 & 0 & 0 \\ 0 & 0 & 0 & 0 & 0 & 1 \end{bmatrix} \tag{2.8}$$

The constraints (2.6) and (2.7), as applied to averages, are rigorous provided t≪h. Their validity can easily be verified from the Eshelby's equivalence principle.

It is evident that the field equations listed above (eqs.(2.1)-(2.4), together with (2.6) and (2.7)) provide a set of 30 equations for 30 unknowns, e.g., $\dot{\sigma}, \dot{\sigma}^{(1)}, \dot{\sigma}^{(2)}, \dot{\epsilon}^{(1)}$ and $\dot{\epsilon}^{(2)}$. Thus, the problem is mathematically determinate. It should be noted that the total number of unknowns can be reduced by introducing certain simplifying assumptions pertaining to the kinematics of bed joints. The formulation discussed by Pietruszczak (1991) for example, has been derived by expressing the local deformation field in bed joints in terms of velocity discontinuities rather than strain rates $\dot{\epsilon}^{(2)}$, thereby reducing the number of unknowns to 27.

In order to solve the problem, i.e., provide an explicit form of the average constitutive relation, it is convenient to introduce the following identity

$$[\delta]\dot{\sigma}^{(i)} = [\delta][D^{(i)}]\dot{e}^{(i)} = [E^{(i)}][\delta^*]\dot{e}^{(i)} + [F^{(i)}][\delta]\dot{e}^{(i)} \quad ; \quad i = 1,2 \tag{2.9}$$

where

$$[E^{(i)}] = \begin{bmatrix} D_{21}^{(i)} & D_{23}^{(i)} & D_{25}^{(i)} \\ D_{41}^{(i)} & D_{43}^{(i)} & D_{45}^{(i)} \\ D_{61}^{(i)} & D_{63}^{(i)} & D_{65}^{(i)} \end{bmatrix} \quad ; \quad [F^{(i)}] = \begin{bmatrix} D_{22}^{(i)} & D_{24}^{(i)} & D_{26}^{(i)} \\ D_{42}^{(i)} & D_{44}^{(i)} & D_{46}^{(i)} \\ D_{62}^{(i)} & D_{64}^{(i)} & D_{66}^{(i)} \end{bmatrix} \tag{2.10}$$

Utilizing eqs(2.9) and (2.6), the static constraint (2.7) can now be expressed in the form

$$[E^{(1)}][\delta^*]\dot{e} + [F^{(1)}][\delta]\dot{e}^{(1)} = [E^{(2)}][\delta^*]\dot{e} + [F^{(2)}][\delta]\dot{e}^{(2)} \tag{2.11}$$

Given the representation (2.11) and the decomposition (2.3), the strain rates in both constituents can be uniquely related to $\dot{\epsilon}$. In view of kinematic constraints (2.6), the set of equations (2.3) reduces to

$$[\delta]\dot{e}^{(2)} = \frac{1}{\eta_2}[\delta]\dot{e} - \frac{\eta_1}{\eta_2}[\delta]\dot{e}^{(1)} \tag{2.12}$$

Substitution of eq.(2.12) in eq.(2.11) results, after a simple algebra, in

$$[\delta]\dot{e}^{(1)} = [\bar{S}]\dot{e} \tag{2.13}$$

where

$$[\bar{S}] = ([F^{(1)}] + \frac{\eta_1}{\eta_2}[F^{(2)}])^{-1}\{\frac{1}{\eta_2}[F^{(2)}][\delta] + ([E^{(2)}] - [E^{(1)}])[\delta^*]\} \tag{2.14}$$

Thus, in view of eq.(2.3), the following relationship is obtained

$$\dot{\epsilon}^{(1)} = [S_1]\dot{\epsilon} \tag{2.15}$$

where

$$[S_1] = \begin{bmatrix} 1 & 0 & 0 & 0 & 0 & 0 \\ \bar{S}_{11} & \bar{S}_{12} & \bar{S}_{13} & \bar{S}_{14} & \bar{S}_{15} & \bar{S}_{16} \\ 0 & 0 & 1 & 0 & 0 & 0 \\ \bar{S}_{21} & \bar{S}_{22} & \bar{S}_{23} & \bar{S}_{24} & \bar{S}_{25} & \bar{S}_{26} \\ 0 & 0 & 0 & 0 & 1 & 0 \\ \bar{S}_{31} & \bar{S}_{32} & \bar{S}_{33} & \bar{S}_{34} & \bar{S}_{35} & \bar{S}_{36} \end{bmatrix} \tag{2.16}$$

and the components of [S] are defined by eq.(2.14).

The strain rates in bed joints can be expressed in a similar functional form to that of eq.(2.15). After substituting eq.(2.15) in eq.(2.3) and solving for $\dot{\epsilon}^{(2)}$, one obtains

$$\dot{\epsilon}^{(2)} = [S_2]\dot{\epsilon} \tag{2.17}$$

where

$$[S_2] = (\frac{1}{\eta_2}[I] - \frac{\eta_1}{\eta_2}[S_1]) \tag{2.18}$$

and [I] represents the unit matrix (6x6).

Finally, the overall stress rate averages σ can be derived form eq.(2.4). Substitution of eqs(2.15) and (2.17) in eq.(2.4), results in

$$\dot{\sigma} = \{\eta_1[D^{(1)}][S_1] + [D^{(2)}]([I]-\eta_1[S_1])\}\dot{\epsilon} = [D]\dot{\epsilon} \tag{2.19}$$

The above equation represents the average constitutive relation for the entire composite system. As expected, the macroscopic behaviour depends on the mechanical properties of both constituents and their volume contributions. In the following sections the proposed mathematical framework is investigated in details. First, the average elastic properties of the masonry are established and subsequently the phenomenon of progressive failure of the material microstructure is addressed.

2.3 AVERAGE ELASTIC PROPERTIES OF STRUCTURAL MASONRY

Assume that all constituents in the microstructure remain elastic and determine the average elastic properties of the composite. Consider first the medium (1), i.e. brick matrix with uniformly dispersed head joints in the form of monotonically aligned rectangular parallelepipeds. If both the bricks and the joints are isotropic then the medium (1), as a whole, will become orthotropic. In this case, the constitutive matrix, eq.(2.1), assumes the form

$$[D^{(1)}] = \begin{bmatrix} D_{11}^{(1)} & D_{12}^{(1)} & D_{13}^{(1)} & 0 & 0 & 0 \\ D_{12}^{(1)} & D_{22}^{(1)} & D_{23}^{(1)} & 0 & 0 & 0 \\ D_{13}^{(1)} & D_{23}^{(1)} & D_{33}^{(1)} & 0 & 0 & 0 \\ 0 & 0 & 0 & D_{44}^{(1)} & 0 & 0 \\ 0 & 0 & 0 & 0 & D_{55}^{(1)} & 0 \\ 0 & 0 & 0 & 0 & 0 & D_{66}^{(1)} \end{bmatrix} \tag{2.20}$$

The nine independent elastic constants are function of the properties of both constituents as well as the cross-sectional aspect ratio and the volume fraction of the inclusions. Recently, Zhao and Weng (1990) have identified the average elastic constants of an orthotropic composite reinforced with aligned elliptic cylinders. The estimates are based on Eshelby's solution to ellipsoidal inclusion problem combined with Mori-Tanaka's mean-field theory (to deal with the finite concentration of inclusions). The results reported by Zhao and Weng can be applied to estimate the average elastic properties of medium (1), viz. eq.(2.20). The algebraic expressions defining the elastic constants are quite complex and will not be cited here. The Reader is referred, in this respect, directly to the original publication.

Assume now that the bed joints, eq.(2.2), are considered as isotropic, i.e.

$$[D^{(2)}] = \begin{bmatrix} D_{11}^{(2)} & D_{12}^{(2)} & D_{12}^{(2)} & 0 & 0 & 0 \\ D_{12}^{(2)} & D_{11}^{(2)} & D_{12}^{(2)} & 0 & 0 & 0 \\ D_{12}^{(2)} & D_{12}^{(2)} & D_{11}^{(2)} & 0 & 0 & 0 \\ 0 & 0 & 0 & D_{44}^{(2)} & 0 & 0 \\ 0 & 0 & 0 & 0 & D_{44}^{(2)} & 0 \\ 0 & 0 & 0 & 0 & 0 & D_{44}^{(2)} \end{bmatrix} ; \quad D_{44}^{(2)} = D_{11}^{(2)} - D_{12}^{(2)} \tag{2.21}$$

Given both representations (2.2) and (2.21) the matrices $[E^{(i)}]$ and $[F^{(i)}]$, defined in eq.(2.10), reduce to

$$[E^{(1)}] = \begin{bmatrix} D_{12}^{(1)} & D_{23}^{(1)} & 0 \\ 0 & 0 & 0 \\ 0 & 0 & 0 \end{bmatrix} ; \quad [F^{(1)}] = \begin{bmatrix} D_{22}^{(1)} & 0 & 0 \\ 0 & D_{44}^{(1)} & 0 \\ 0 & 0 & D_{66}^{(1)} \end{bmatrix} \tag{2.22}$$

$$[E^{(2)}] = \begin{bmatrix} D_{12}^{(2)} & D_{12}^{(2)} & 0 \\ 0 & 0 & 0 \\ 0 & 0 & 0 \end{bmatrix} ; \quad [F^{(2)}] = \begin{bmatrix} D_{11}^{(2)} & 0 & 0 \\ 0 & D_{44}^{(2)} & 0 \\ 0 & 0 & D_{44}^{(2)} \end{bmatrix} \tag{2.23}$$

Substituting the above representation in eq.(2.14), one obtains after some algebraic manipulations

$$[\bar{S}] = \begin{bmatrix} \dfrac{(D_{12}^{(2)}-D_{12}^{(1)})}{a} & \dfrac{D_{11}^{(2)}}{\eta_2 a} & \dfrac{(D_{12}^{(2)}-D_{23}^{(1)})}{a} & 0 & 0 & 0 \\ 0 & 0 & 0 & \dfrac{D_{44}^{(2)}}{\eta_2 b} & 0 & 0 \\ 0 & 0 & 0 & 0 & 0 & \dfrac{D_{44}^{(2)}}{\eta_2 c} \end{bmatrix} \tag{2.24}$$

where

$$a = D_{22}^{(1)} + \frac{\eta_1}{\eta_2} D_{11}^{(2)} \quad ; \quad b = D_{44}^{(1)} + \frac{\eta_1}{\eta_2} D_{44}^{(2)} \quad ; \quad c = D_{66}^{(1)} + \frac{\eta_1}{\eta_2} D_{44}^{(2)}$$

Thus, given the definitions (2.20), (2.21) and (2.24), the components of the macroscopic constitutive matrix can be determined from eq.(2.19). The composite panel is an orthotropic body (on a macroscale) and the nine independent components of [D] matrix are defined as

$$D_{11} = (\eta_1 D_{11}^{(1)}+\eta_2 D_{11}^{(2)}) - \frac{\eta_1 (D_{12}^{(2)}-D_{12}^{(1)})^2}{D_{22}^{(1)}+\frac{\eta_1}{\eta_2}D_{11}^{(2)}} \; ; \quad D_{22} = \frac{1}{\frac{1}{\eta_1}D_{22}^{(1)}+\frac{1}{\eta_2}D_{11}^{(2)}}$$

$$D_{33} = (\eta_1 D_{33}^{(1)}+\eta_2 D_{11}^{(2)}) - \frac{\eta_1 (D_{12}^{(2)}-D_{23}^{(1)})^2}{D_{22}^{(1)}+\frac{\eta_1}{\eta_2}D_{11}^{(2)}} \; ; \quad D_{44} = \frac{1}{\frac{1}{\eta_1}D_{44}^{(1)}+\frac{1}{\eta_2}(D_{11}^{(2)}-D_{12}^{(1)})}$$

$$D_{55} = \eta_1 D_{55}^{(1)}+\eta_2 (D_{11}^{(2)}-D_{12}^{(2)}) \; ; \quad D_{66} = \frac{1}{\frac{1}{\eta_1}D_{66}^{(1)}+\frac{1}{\eta_2}(D_{11}^{(2)}-D_{12}^{(2)})}$$

$$D_{12} = (\eta_1 D_{12}^{(1)}+\eta_2 D_{12}^{(2)}) - \frac{\eta_1 (D_{12}^{(2)}-D_{12}^{(1)})(D_{11}^{(2)}-D_{22}^{(2)})}{D_{22}^{(1)}+\frac{\eta_1}{\eta_2}D_{11}^{(2)}} \tag{2.25}$$

$$D_{13} = (\eta_1 D_{13}^{(1)}+\eta_2 D_{12}^{(2)}) - \frac{\eta_1 (D_{12}^{(2)}-D_{12}^{(1)})(D_{12}^{(2)}-D_{23}^{(1)})}{D_{22}^{(1)}+\frac{\eta_1}{\eta_2}D_{11}^{(2)}}$$

$$D_{23} = (\eta_1 D_{23}^{(1)}+\eta_2 D_{12}^{(2)}) - \frac{\eta_1 (D_{12}^{(2)}-D_{23}^{(1)})(D_{11}^{(2)}-D_{22}^{(1)})}{D_{22}^{(1)}+\frac{\eta_1}{\eta_2}D_{11}^{(2)}}.$$

In order to illustrate the mathematical framework outlined in this section, some numerical simulations were carried out. The objective was to investigate the influence of the joint thickness and the elastic properties of the constituents (brick and mortar) on the average elastic response of the masonry panel. Both constituents were assumed to be isotropic and the elastic constants (Young's modulus, E and Poisson's ratio, ν) were selected after Pande et al. (1989) as

$E_b = 1.1 \times 10^4$ MPa; $\nu_b = 0.25$; $\nu_m = 0.20$

where the subscripts b and m refer to brick and mortar, respectively. The brick dimensions were taken as: h=75 mm, l=225 mm.

Fig.2.2 shows the variation of nine elastic constants (normalised with respect to the properties of the brick) of the masonry panel as a function of the thickness, t, of the joints. The simulations were carried out for different E_b/E_m ratios ranging from 1.1 to 11. It is evident, from the figure 2.2, that an increase in the joint thickness results in a progressive reduction of average elastic moduli (E and G), whereas an increase of the Young's modulus of the mortar causes a corresponding increase in these values.

The contribution of the head joints to the average macroscopic properties of the masonry panel is investigated further in Figs.2.3 and 2.4. The results shown in Fig.2.3 correspond to the case in which the head joints are treated as continuous vertical planes of weakness ($\alpha \to 0$, where α is the cross sectional aspect ratio of the head joints, Zhao and Weng, 1990). In other words, the masonry panel is regarded as an elastic medium intercepted by two mutually orthogonal families of continuous joints. The latter approximation was employed by Pande et al.(1989) to estimate the average elastic properties of masonry through a direct strain energy approach. By comparing the results with those in Fig.2.2, it is evident that the predictions are very close and only the values of E_{11} and G_{31} are underestimated. Thus, the treatment of head joints as weakness planes provides a reasonable approximation in the context of the elastic response of the system.

Finally, Fig.2.4 shows the most conservative prediction corresponding to the case when the head joints are infilled, i.e. are regarded as voids ($E_m \to 0$). The values of the overall moduli (E and G) are, in general, reduced as compared to those in Fig.2.2, in particular E_{11} and G_{31} are affected. It is clear however, that the masonry structure with head joints infilled is still capable of resisting the external load.

2.4 DESCRIPTION OF PROGRESSIVE FAILURE OF STRUCTURAL MASONRY

The collapse of a masonry panel can result either from the failure of the brick matrix, which is usually of a brittle nature, or from the ductile/brittle failure of the bed joints. The head joints represent a less significant link in the panel microstructure, in the sense that their local failure will not induce the collapse on a macroscale. Thus, it seems reasonable to regard the medium (1) as an orthotropic elastic body, eq.(2.20), and impose an appropriate criterion for the elastic-brittle transition in the bricks. At the same time, the bed joints can be treated as an elastoplastic strain-hardening material.

Consider first the homogenized medium (1). In order to determine the stress rates in the bricks, express the averaging procedure, eqs(2.3) and (2.4), as

$$\dot{\sigma}^{(1)} = \eta'\dot{\sigma}' + \eta''\dot{\sigma}'' \tag{2.26}$$

$$\dot{\epsilon}^{(1)} = \eta'\dot{\epsilon}' + \eta''\dot{\epsilon}'' \tag{2.27}$$

Here, the prime and double prime superscripts refer to brick matrix and mortar (head) joints respectively, whereas η's are the volume fractions of both constituents

$$\eta' = \frac{l}{l+t} \quad ; \quad \eta'' = \frac{t}{l+t} \tag{2.28}$$

where l represents the spacing of the head joints.

With all the constituents remaining elastic, i.e.,

$$\dot{\sigma}' = [D']\dot{\epsilon}' \quad ; \quad \dot{\sigma}'' = [D'']\dot{\epsilon}'' \quad ; \quad \dot{\sigma}^{(1)} = [D^{(1)}]\dot{\epsilon}^{(1)} \tag{2.29}$$

the stress decomposition, eq.(2.26), yields

$$[D^{(1)}]\dot{\epsilon}^{(1)} = \eta'[D']\dot{\epsilon}' + \eta''[D'']\dot{\epsilon}'' \tag{2.30}$$

Thus, substituting eq.(2.27) in eq.(2.30) and rearranging

$$\dot{\epsilon}' = [S']\dot{\epsilon}^{(1)} \quad ; \quad [S'] = \frac{1}{\eta'}([D']-[D''])^{-1}([D^{(1)}]-[D'']) \tag{2.31}$$

so that the stress rates in the brick matrix are defined as

$$\dot{\sigma}' = [D']\dot{\epsilon}' = [D'][S']\dot{\epsilon}^{(1)} \tag{2.32}$$

The failure criterion for the bricks can be expressed in terms of a path-independent condition

$$F(\sigma') = 0 \tag{2.33}$$

in which F=0 is a scalar-valued function of the basic invariants of σ'. In particular, the functional form proposed by Pietruszczak et al.(1988) may be used

$$F = a_1\left(\frac{\sqrt{J_2}}{g(\theta)f_c}\right) + a_2\left(\frac{\sqrt{J_2}}{g(\theta)f_c}\right)^2 - \left(a_3 - \frac{I}{f_c}\right) = 0 \tag{2.34}$$

where I is the first stress invariant, J_2 is the second invariant of the stress deviator and θ is the angle measure of the third deviatoric stress invariant J_3,

$$\theta = \frac{1}{3}\sin^{-1}\left(\frac{-3\sqrt{3}}{2}\frac{J_3}{J_2^{3/2}}\right) ; \quad -\frac{\pi}{6} \leq \theta \leq \frac{\pi}{6} \tag{2.35}$$

The parameter a_1 through a_3 are dimensionless material constants, whereas f_c represents uniaxial compressive strength of the brick. The function $g(\theta)$, eq.(2.34), can be selected in the form

$$g(\theta) = \frac{(\sqrt{(1+a)}-\sqrt{(1-a)})K}{K\sqrt{(1+a)}-\sqrt{(1-a)}+(1-K)\sqrt{(1-sin3\theta)}} ; K = 1-K_0 e^{-K_1(a_3-I/f_c)} \tag{2.36}$$

which satisfies $g(\pi/6)=1$, $g(-\pi/6)=K$ and for $a=0.999$ guaranties convexity for $K>0.56$.

Consider now the response of the bed joints. Assuming that joints are elastoplastic, the components of $[D^{(2)}]$, eq.(2.2), can be derived from the standard plasticity formulism based on the existence of yield and plastic potential functions

$$f = f(\sigma^{(2)},\kappa) = 0 \quad ; \quad \psi = \psi(\sigma^{(2)}) = const \tag{2.37}$$

where κ is a scalar parameter recording the history of plastic deformation, i.e., $\kappa=\kappa\{(\epsilon^{(2)})^p\}$. In particular, the properties of the mortar can be described by one of the existing formulations applicable to brittle-plastic materials (see e.g., Chen and Han, 1988; Pietruszczak et al., 1988).

By inspecting the geometry of typical structural panels, it is evident that the thickness of bed joints is small as compared to other dimensions. In such a case, the analysis may be simplified by assuming both expressions (2.37) in the functional form

$$\begin{aligned} f &= \sqrt{(\sigma_{12}^{(2)})^2 + (\sigma_{23}^{(2)})^2} - \mu(\sigma_{22}^{(2)} + c) = 0 . \\ \psi &= \sqrt{(\sigma_{12}^{(2)})^2 + (\sigma_{23}^{(2)})^2} - \bar{\mu}\sigma_{22}^{(2)} = const \end{aligned} \tag{2.38}$$

which is analogous to Coulomb friction law. In eq.(2.38), $\mu = \mu(\xi)$, where ξ is a suitably chosen hardening parameter. In particular, one can select

$$\mu = \mu_0 + (\mu_f - \mu_0)\frac{\xi}{\xi+\alpha} \quad ; \quad \xi = \sqrt{[(\gamma_{12}^{(2)})^p]^2 + [(\gamma_{23}^{(2)})^p]^2} \tag{2.39}$$

where μ_0, μ_f and α are material constants. Equations (2.38) and (2.39) are sufficient to define, in a unique manner, the components of $[D^{(2)}]$, eq.(2.2), by following a routine plasticity procedure.

In order to verify the performance of the proposed framework, an extensive numerical study was undertaken. In particular, a series of in-plane biaxial compression-tension and compression-compression tests was simulated for different orientations of the set of bed joints relative to loading configuration. The analysis was carried out assuming the brick dimensions as 215 mm x 65 mm and the thickness of the joints as 10 mm. The following material parameters were chosen:

Brick: $E_b = 14{,}700$ MPa, $\nu_b = 0.16$, $f_c = 15.3$ MPa, $f_t = 1.2$ MPa

Mortar: $E_m = 7{,}400$ MPa, $\nu_m = 0.21$

$\mu_f = 0.73$, $\mu_0 = 0.3\mu_f$, $\mu = 0.2\mu_f$, $c = 0.78$ MPa, $\alpha = 0.001$

The material constants describing the response in the elastic range were assumed after Ali and Page (1989). The same reference was used to estimate the values of the last set of parameters, pertaining to the elastoplastic behaviour of mortar. The choice of μ_0, μ and α has been somewhat arbitrary due to the limited experimental information.

Fig.2.5 shows a set of failure envelopes obtained from the simulation of a series of in-plane biaxial compression-tension tests. The loading process involved a number of trajectories corresponding to a constant compressive- tensile stress ratio (i.e., 0, 0.25, 0.5, 0.75, 1, 2, 5, 10, 30, ∞). The simulations were successively repeated for different orientations of bed joints relative to the direction of the tensile stress (the angle β, ranging from 0° to 90°).Fig.2.5, apart from defining the set of failure envelopes, provides a direct information on the failure mode pertaining to each individual loading history. For low values of β (i.e., $\beta=0°$ and $\beta=22.5°$) the collapse of the brickwork is solely induced by the brittle failure of bricks. For $45° < \beta < 78.75°$, the predominant mechanism is the failure of the bed joints, whereas for $\beta=33.75°$ and $\beta=90°$ both modes are possible depending on the actual stress ratio.

Fig.2.6 presents the evolution of uniaxial compressive and tensile strength of the brickwork with varying orientation of the bed joints. The results, which are extracted from Fig.2.5, indicate that the ultimate strength (both in compression and tension) is the highest for low values of β, i.e., when the failure of masonry is induced by brittle rupture of bricks. As β increases a transition in the failure mode takes place which prompts a drastic reduction in the uniaxial strength. The lowest value corresponds to $\beta \approx 60°$ (bed joint failure).

The results shown in Fig.2.5 and 2.6 describe the conditions at failure only, i.e., identify the maximum stress ratio which can be attained for a given stress history. For each loading case, a complete stress-strain characteristics are obtained by integration of the constitutive law (2.19). As an illustration, one such a characteristics, corresponding to $\beta=45°$ and stress ratio of 5.0, is presented in Fig.2.7. A complete deformation history, both on a macroscale and for all the individual constituents, is recorded. Here, the failure of the masonry panel is induced by a ductile failure (shearing) of the bed joints.

The results shown in Fig.2.8 correspond to a series of in-plane biaxial compression-compression tests. The loading program was analogous to that for compression-tension and involved a number of stress trajectories at constant vertical to horizontal stress ratio. In this case, the predominant failure mechanism is associated with the brittle failure of the brick matrix. The failure of bed joints is recorded only for some cases involving extremal values of the stress ratio.

The last aspect of the present analysis is the evaluation of the influence of head joints on the macroscopic failure. The predictions shown in Fig.2.5-2.8 have all been based on the assumption that the head joints are linearly elastic. This assumption may not be quite adequate as certain stress trajectories may result in the failure of head joints. Fig.2.9 shows the prediction for two chosen biaxial tests obtained for the case when the head joints are treated as infilled. Comparing both solutions, i.e., for elastic and infilled head joints, it is evident that the conditions at failure are only marginally affected by the treatment of head joints. In fact, when the failure is initiated in bed joints, the predictions are virtually the same, only when the bricks fail, the predictions show some degree of sensitivity.

Finally, it should be stressed that the numerical analysis presented here is, in fact, of a qualitative nature as no comparison to the experimental data has been provided. The reason is that the experimental reports are usually very fragmentary and there is no comprehensive study giving an adequate information required for a quantitative study. It should be noted however that the qualitative trends presented here, in the context of both compression-tension and compression-compression tests, are in a close agreement with experimental results reported by Page (1981 and 1983).

2.5 CONCLUSIONS

A mathematical formulation has been presented for describing the average properties of the structural masonry. The approach has been derived from the framework of the mechanics of composite media. The proposed constitutive law (2.9) relates, in a unique manner, the stress rate σ to strain rate ϵ averages. Their local counterparts are derived from the corresponding global measures by means of structural matrices whose components are function of properties of both constituents and their volume contributions. The framework can be incorporated into exiting numerical packages to analyze masonry panels of arbitrary geometry. This is feasible providing the characteristic dimension of the elementary volume is much greater than the predominant dimension of the masonry unit.

It has been shown that in the elastic range the brickwork can be considered as an orthotropic medium. The values of elastic constants are strongly influenced by the properties and the thickness of the mortar joints. The failure mechanism consists of a formation of macrocracks in brick matrix or a ductile/brittle failure of the bed joints. The actual failure mode is a function of the imposed loading history. The properties of the head joints have a very limited effect on the macroscopic failure. Thus, for practical purpose, the head joints may be assumed as isotropic linearly elastic.

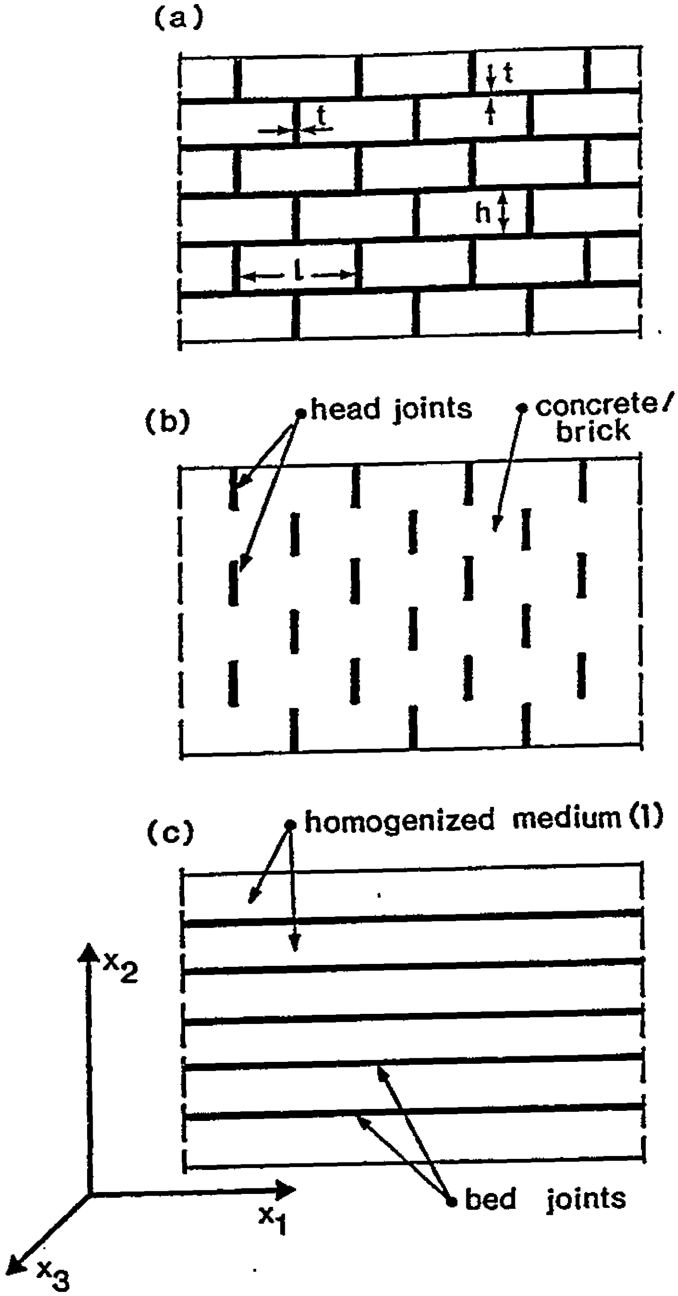

Fig.2.1 (a) Geometry of a structural masonry panel; (a) medium (1); (c) medium (1) intercepted by bed joints (after Pietruszczak, 1991).

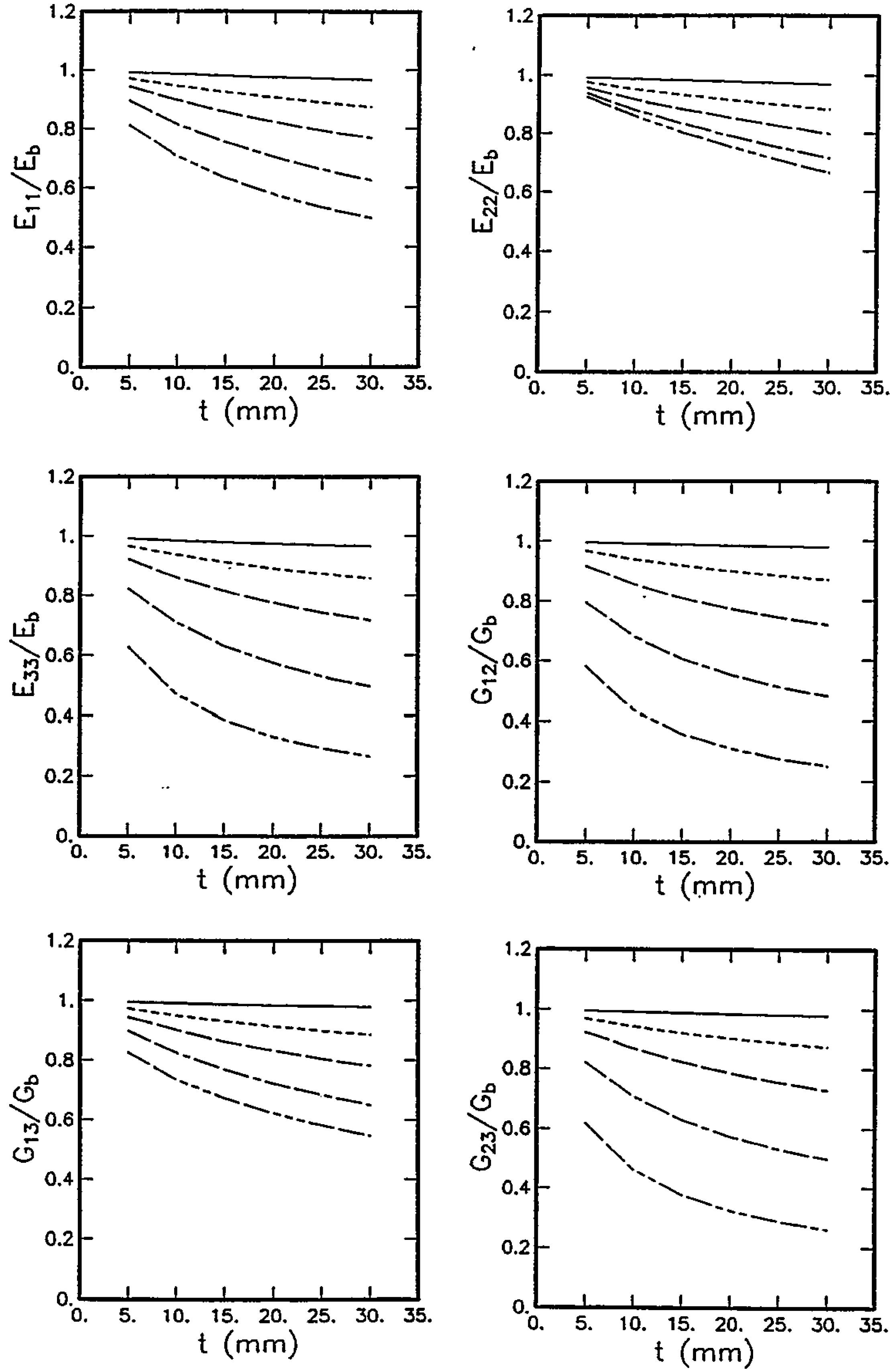

E11/Eb
E22/Eb
E33/Eb
G12/Gb
G13/Gb
G23/Gb
t (mm)
0. 5. 10. 15. 20. 25. 30. 35.
0. 0.2 0.4 0.6 0.8 1. 1.2

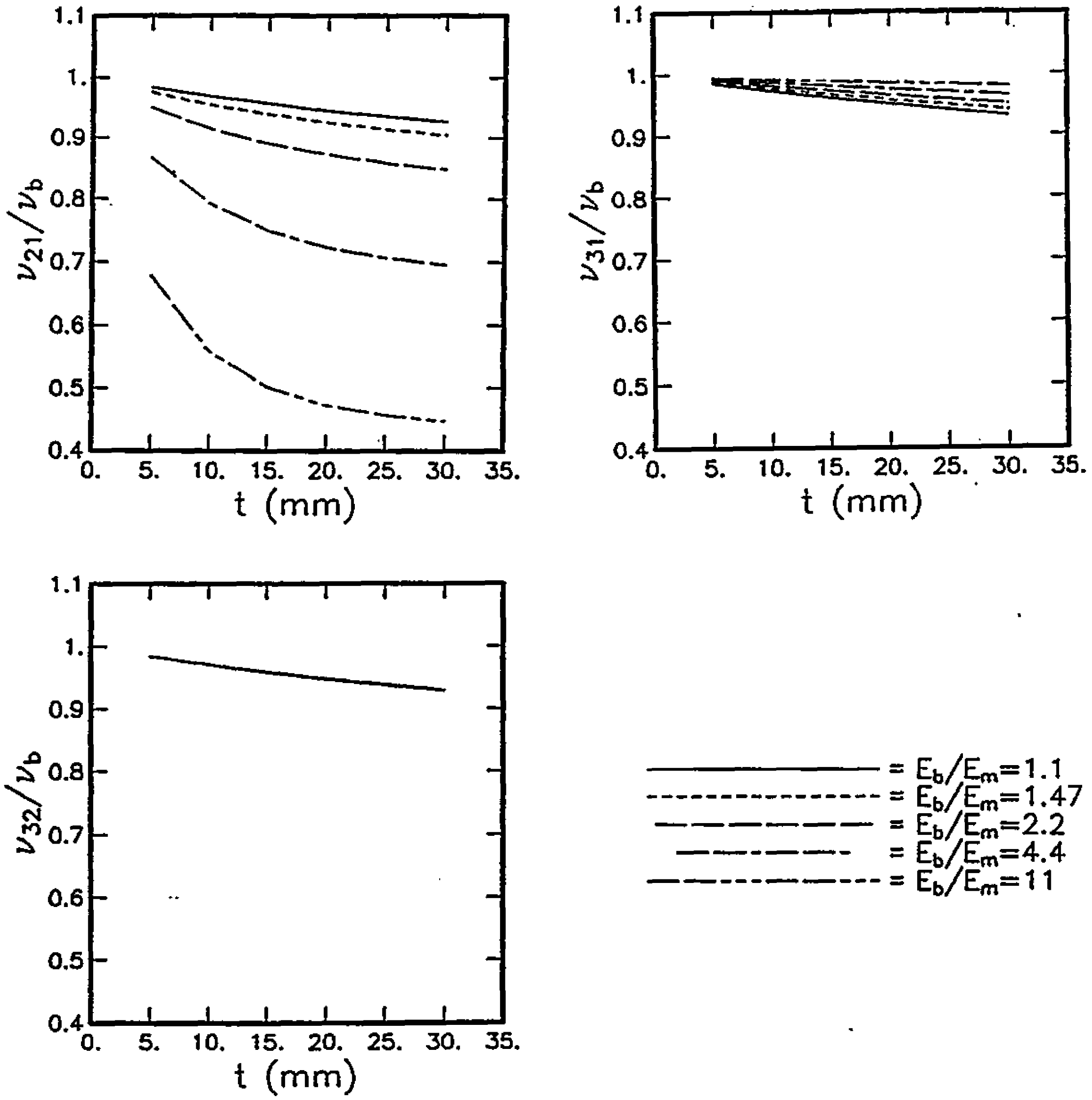

Fig.2.2 Average elastic properties of structural masonry.

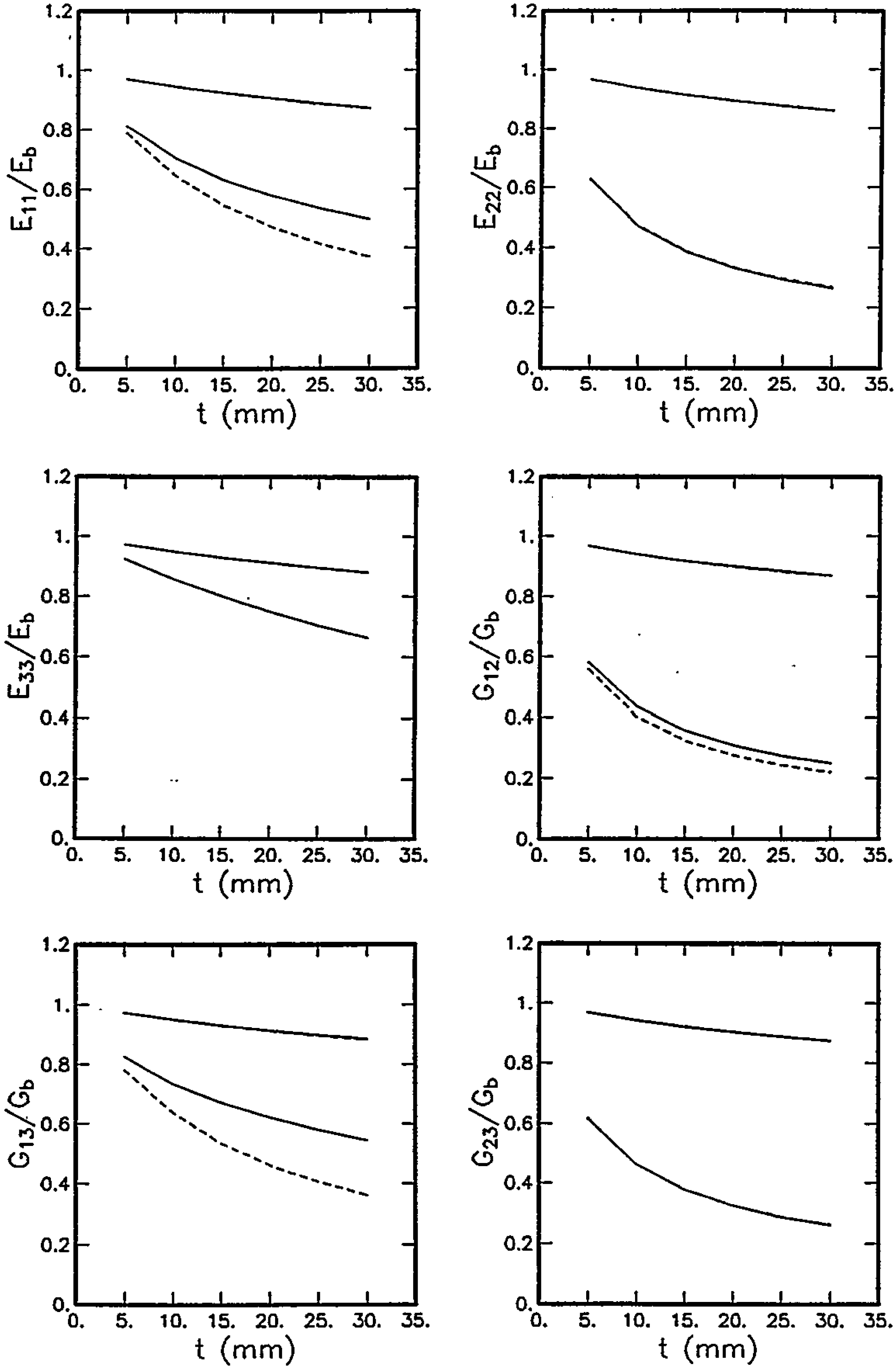
E_{11}/E_b
t (mm)
E_{22}/E_b
t (mm)
E_{33}/E_b
t (mm)
G_{12}/G_b
t (mm)
G_{13}/G_b
t (mm)
G_{23}/G_b
t (mm)

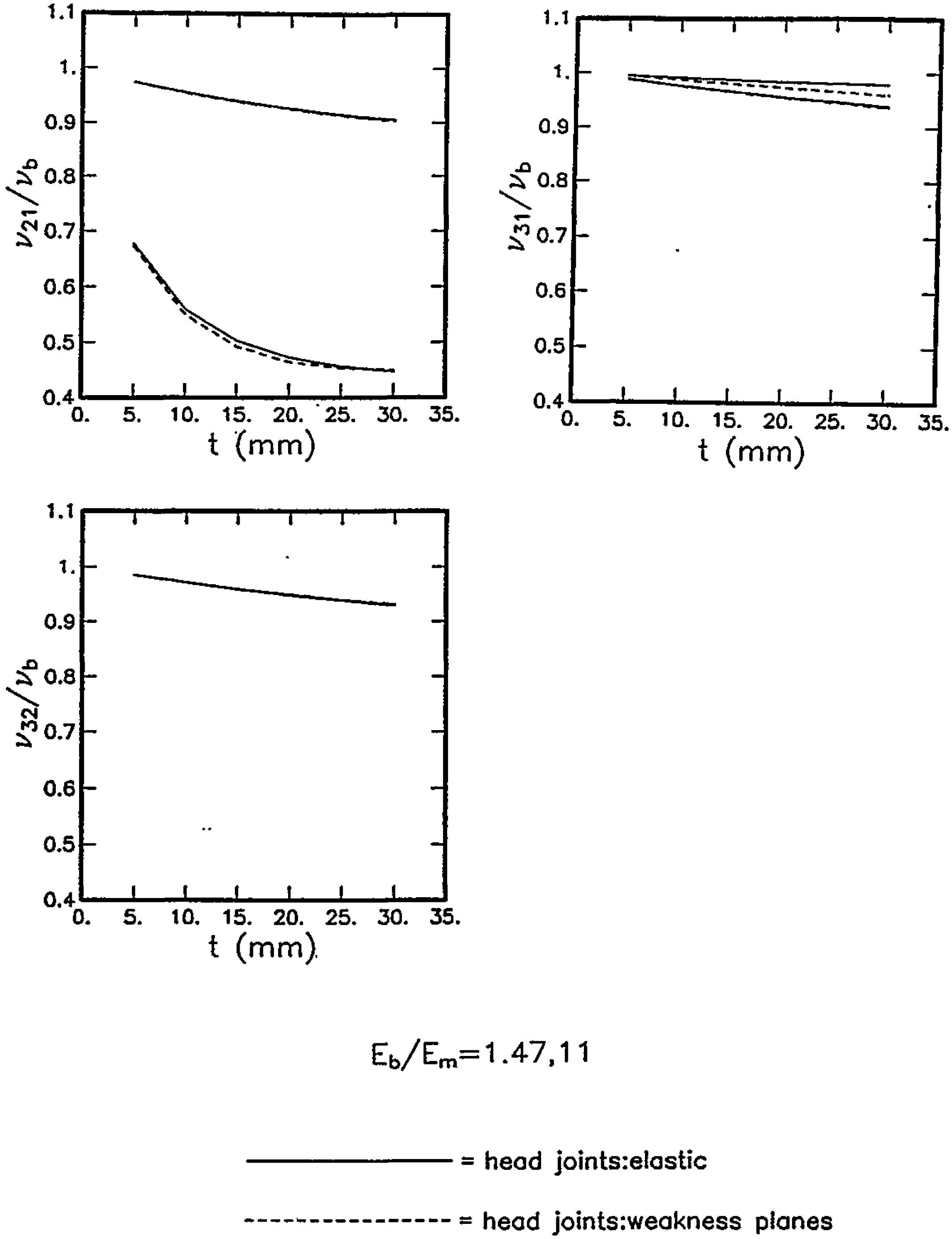

Fig.2.3 Influence of the head joints on the average elastic properties of masonry.

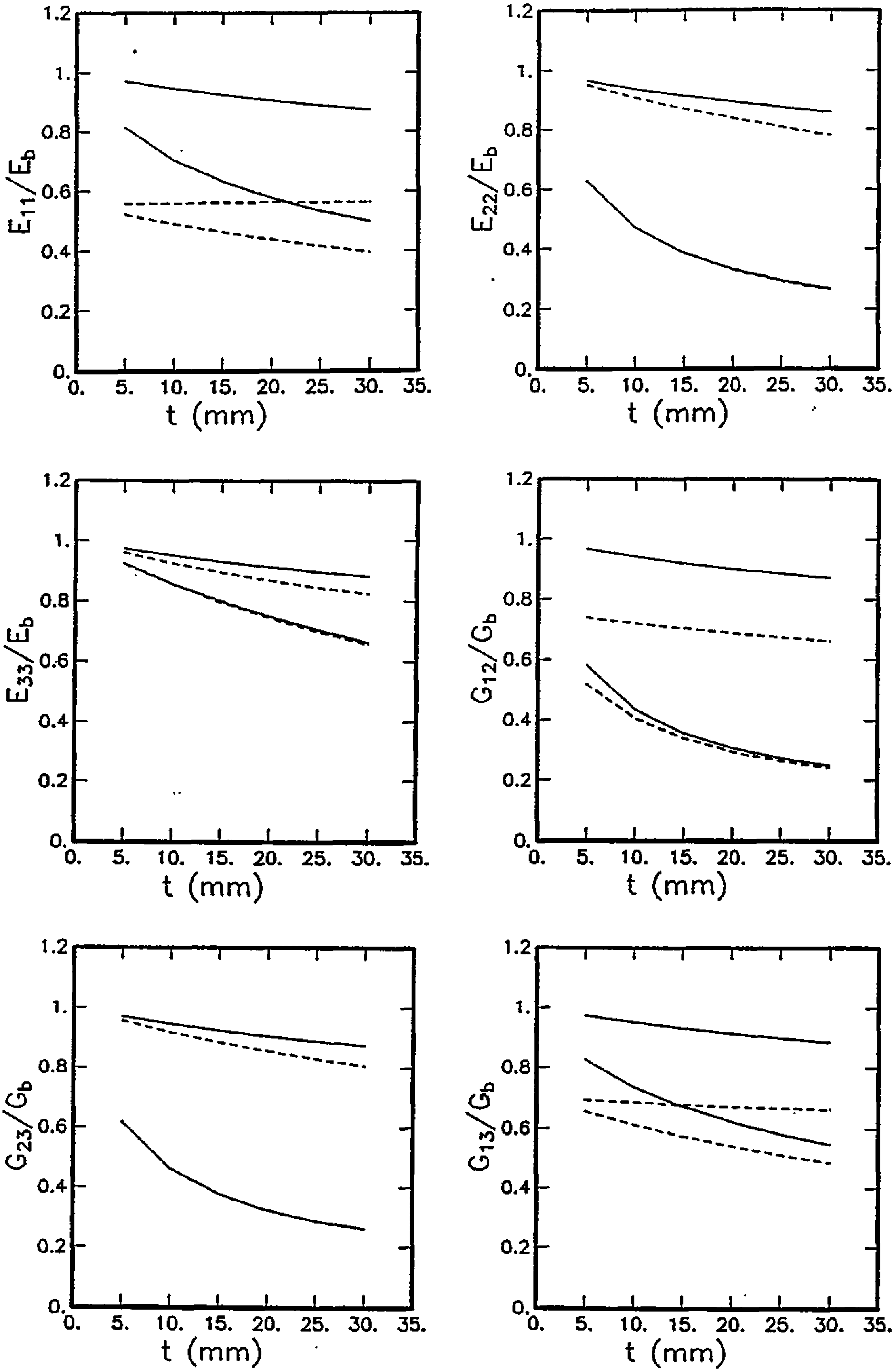

E_{11}/E_b
E_{22}/E_b
E_{33}/E_b
G_{12}/G_b
G_{23}/G_b
G_{13}/G_b
t (mm)
0. 5. 10. 15. 20. 25. 30. 35.
0. 0.2 0.4 0.6 0.8 1. 1.2

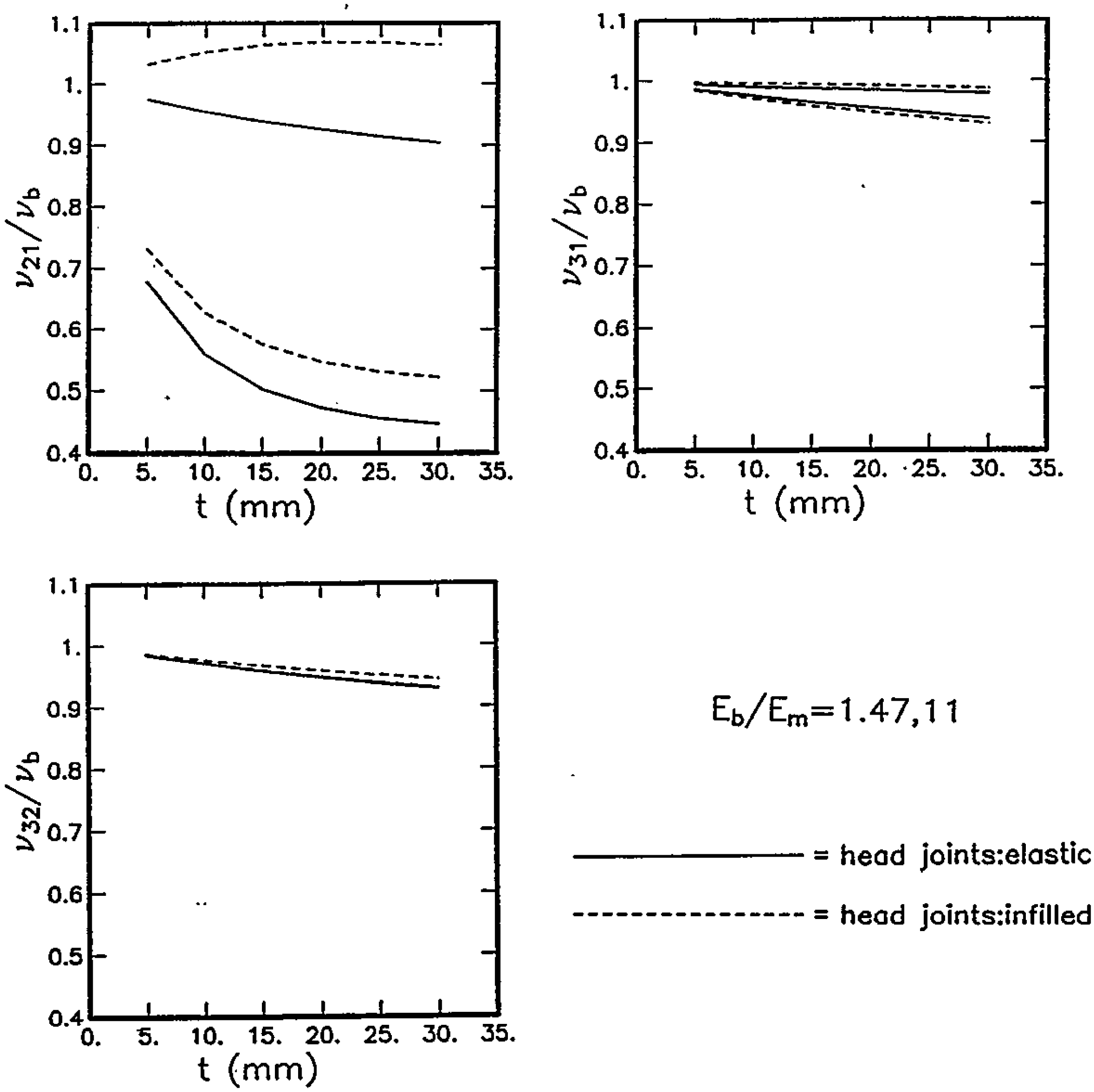

Fig.2.4 Influence of the head joints on the average elastic properties of masonry.

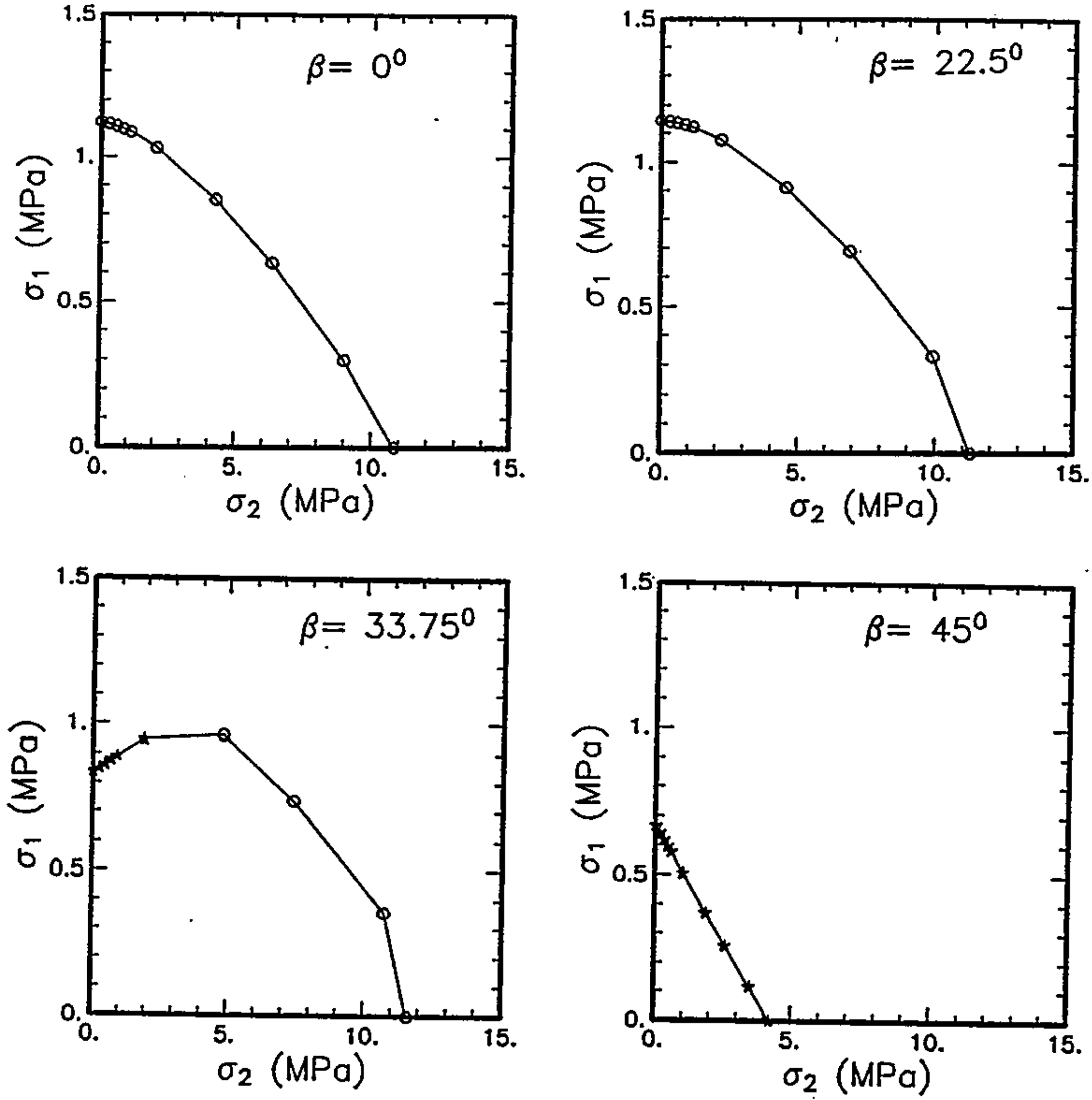

β= 0⁰
β= 22.5⁰
β= 33.75⁰
β= 45⁰
σ_1 (MPa)
σ_2 (MPa)
0.
0.5
1.
1.5
0.
5.
10.
15.

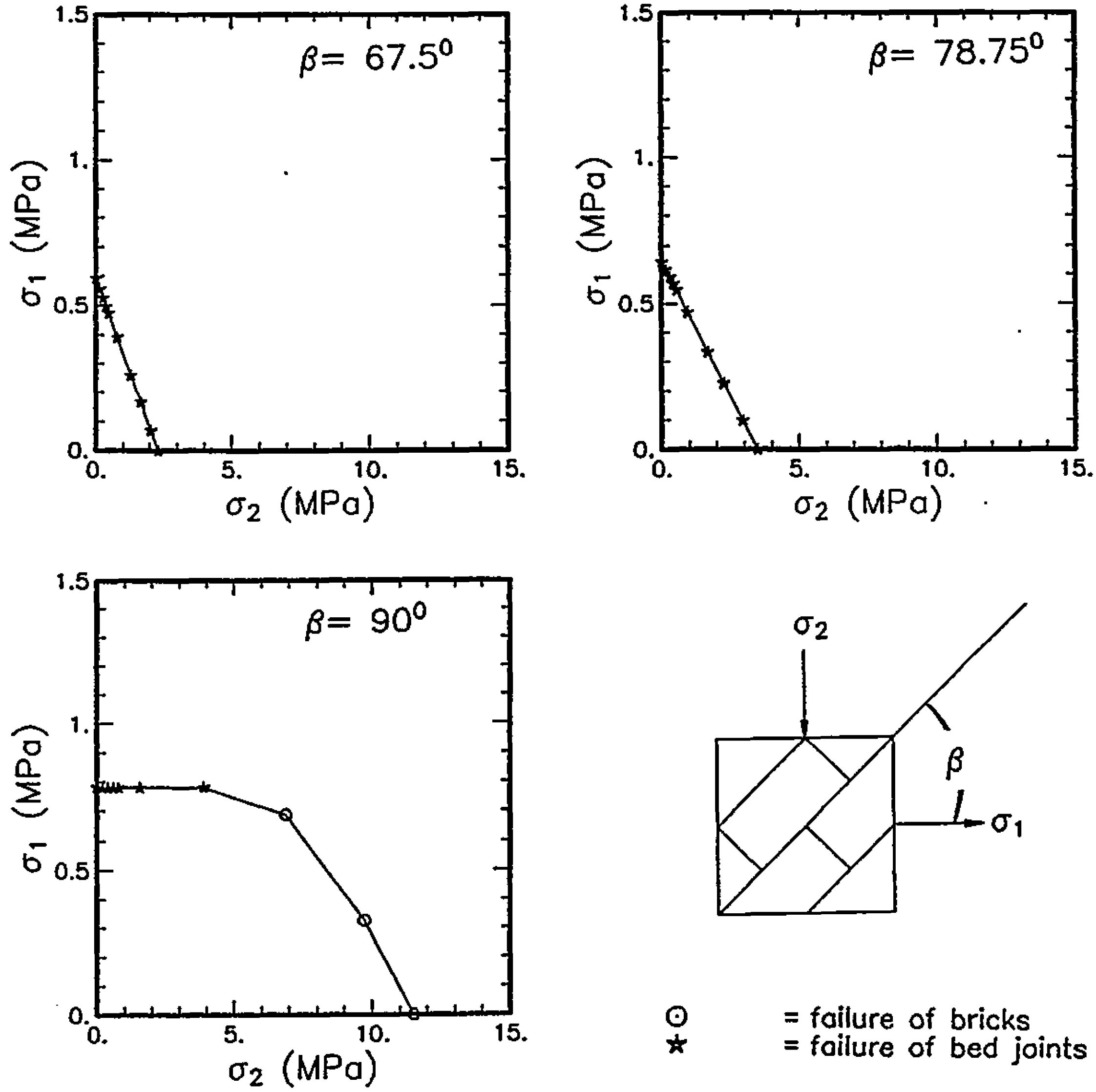

Fig.2.5 Failure envelopes for in-plane biaxial compression-tension test.

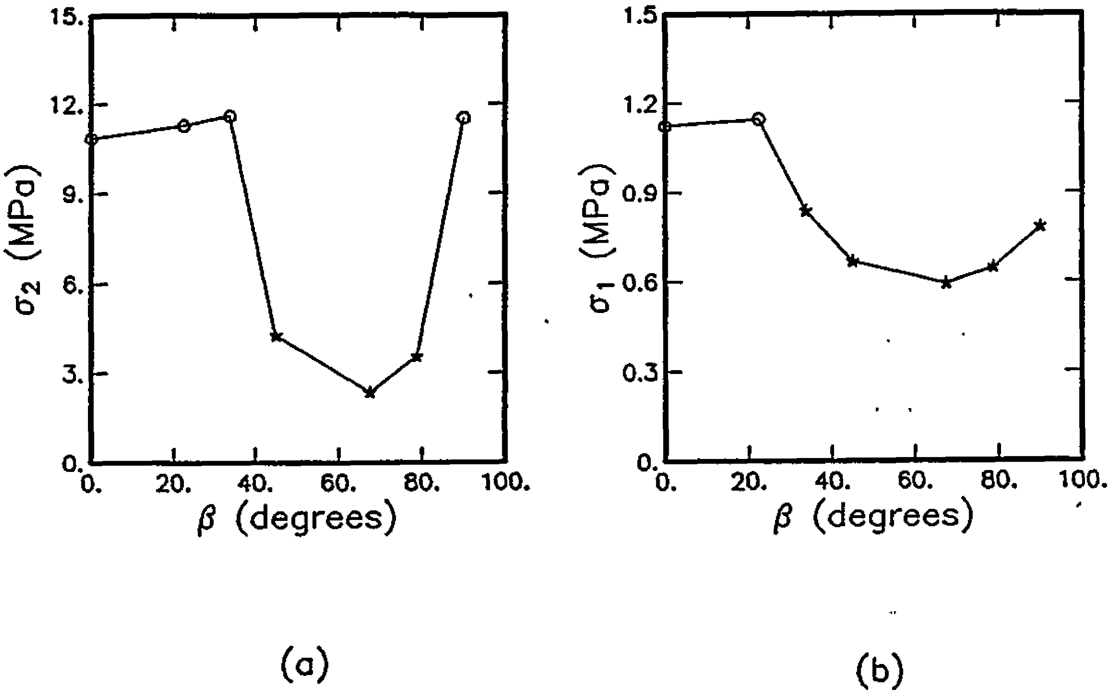

Fig.2.6 Variation of uniaxial compressive (a) and tensile (b) strength with the orientation of bed joints.

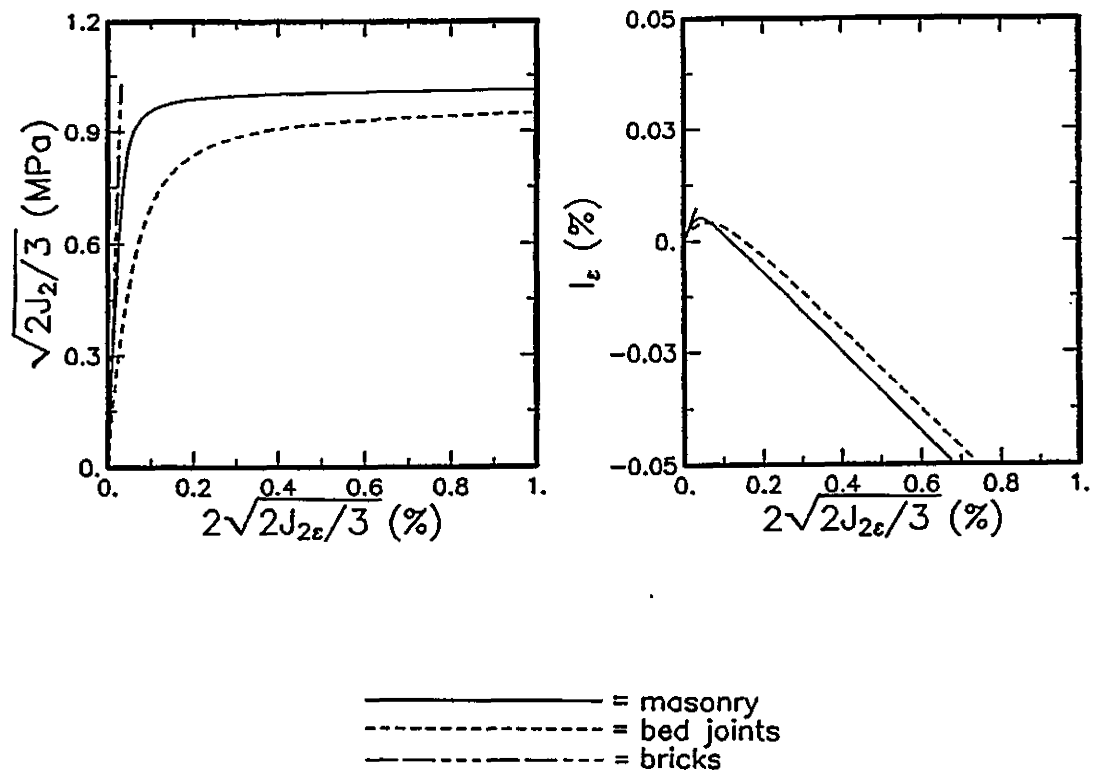

Fig.2.7 Material characteristics corresponding to biaxial compression test ($\beta = 45^0$; stress ratio:5.0).

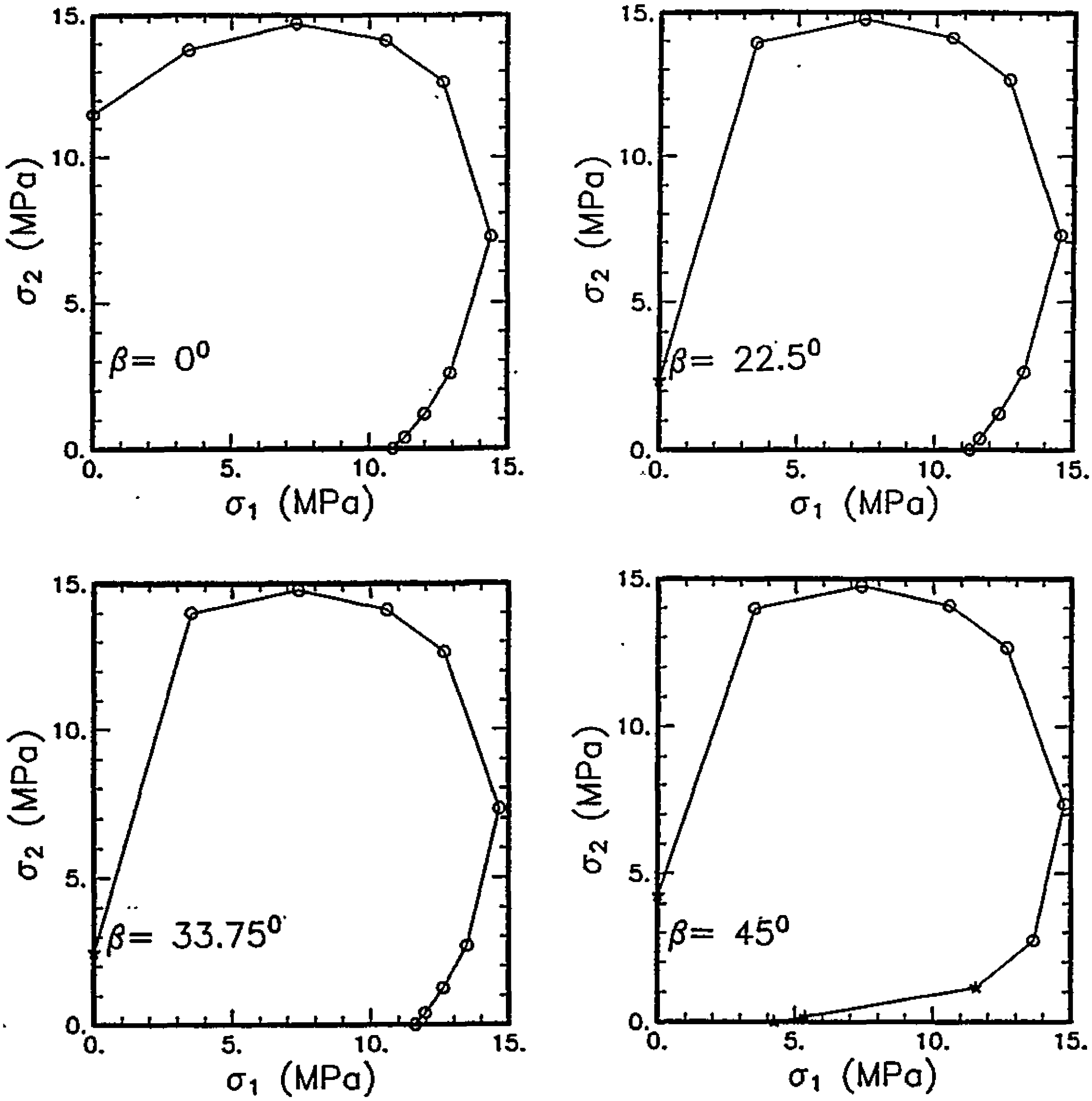

$\beta = 0^0$
$\beta = 22.5^0$
$\beta = 33.75^0$
$\beta = 45^0$
σ_2 (MPa)
σ_1 (MPa)
0.
5.
10.
15.

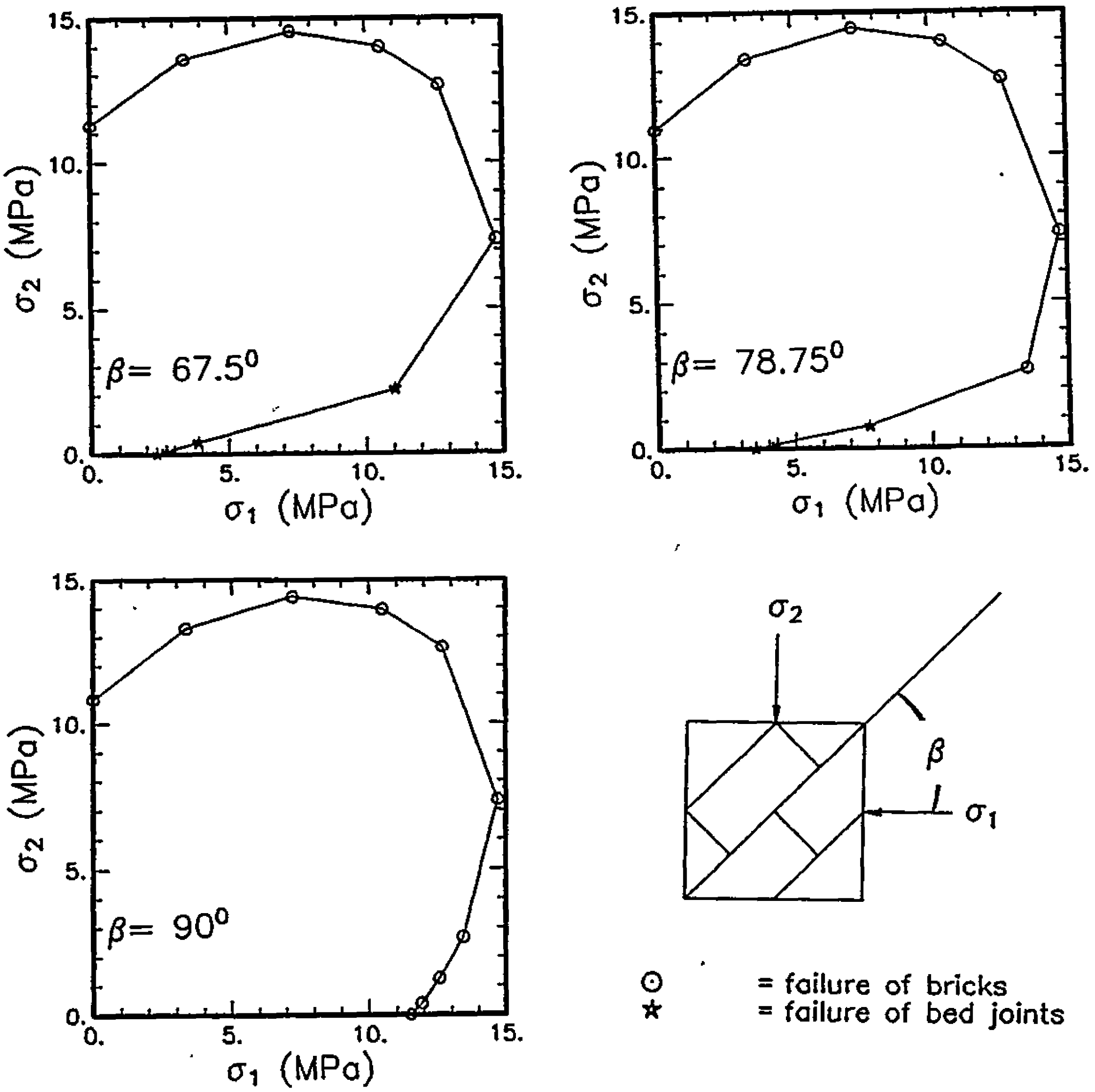

Fig.2.8 Failure envelopes for in-plane biaxial compression tests.

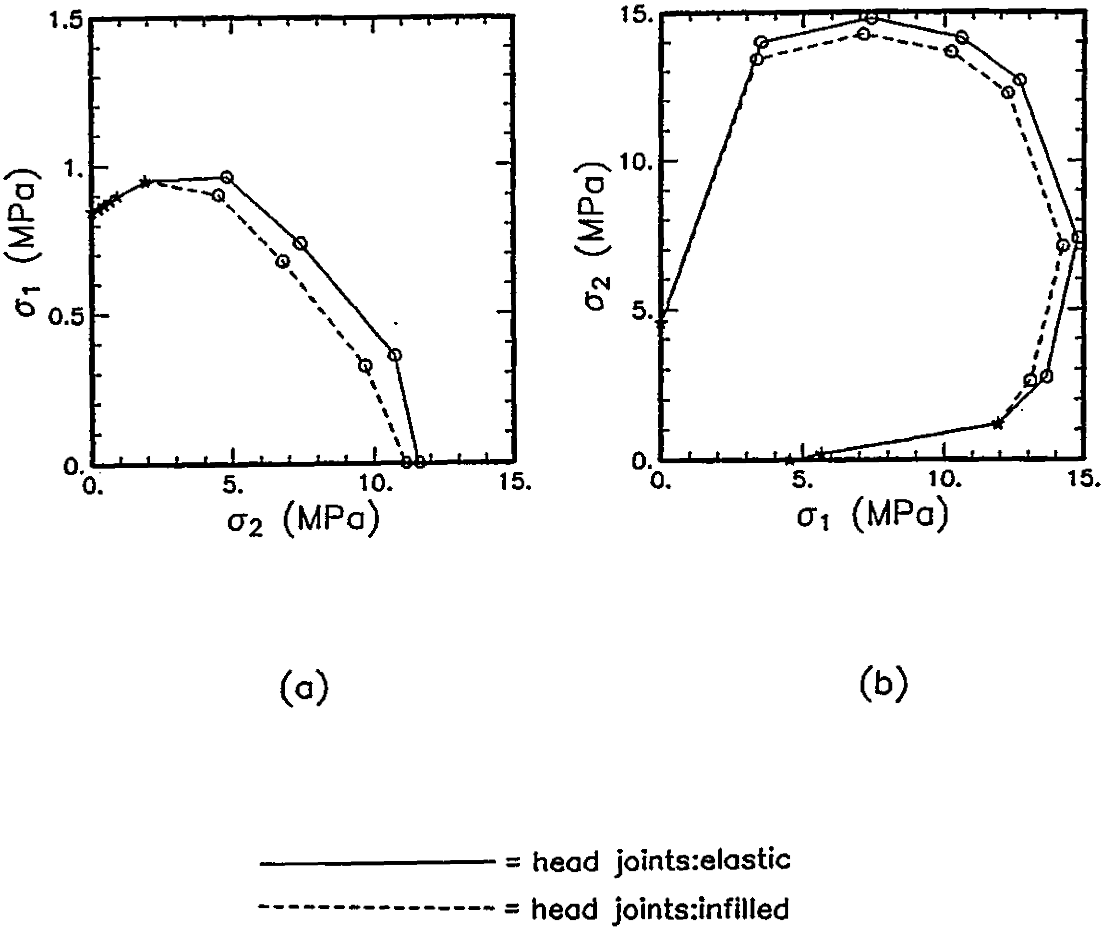

Fig.2.9 Influence of head joints on the response under biaxial conditions (a) biaxial compression-tension; (b) biaxial compression.

CHAPTER 3

MACROSCOPIC DESCRIPTION OF ELASTOPLASTIC BEHAVIOUR OF PERFECTLY BONDED COMPOSITES

3.1 INTRODUCTION

Composite materials, such as metal and thermoplastic composites, can experience significant elastoplastic deformations. Since the reinforcement usually remains elastic up to failure, the nonlinearity of a composite system results from the inelastic behaviour of the matrix.

The methodologies adopted in the past few decades for the description of the elastoplastic response of composite systems can be classified into two categories. In the first one, a composite system is regarded as a homogenous isotropic/anisotropic medium. The overall mechanical properties are derived on the basis of experiments recording the overall stress-strain response (Kenaga, Doyle and Sun, 1987). The advantage of this approach is its simplicity but in return the macroscopic stress-strain description of the composite cannot be related to the mechanical properties of its constituents. On the other hand, the micro-mechanical approach is able to address this problem by retaining the identities of the reinforcement and the matrix. Thus, a macroscopic model can be established in which the overall constitutive equation depends on the mechanical characteristics of the constituents, the respective volume contributions as well as the mutual constraints between interfaces of the constituents associated with the geometry of the microstructure (Dvorak and Bahei-El-Din, 1979; Dvorak and Bahei-El-Din, 1982; Tandon and Weng, 1988). In addition, the finite element method can be employed to analyze a typical element of a composite system in order to obtain some information about the elastoplastic behaviour under chosen loading conditions (Adams, 1973; Lin, Salinas and Ito, 1972).

This chapter presents a micro-mechanical approach for the description of fibre/particle reinforced composite systems. The methodology followed is based on the concept of a "superimposed medium" used elsewhere (Pande, Liang and Middleton, 1989; Pietruszczak, 1991; Pietruszczak and Niu, 1991). In this approach, the elastic properties and the elastoplastic response of both fibre and particle reinforced composites can be addressed under a unified framework. Numerical simulations, pertaining to the evaluation of elastic constants of fibre and particle reinforced composites as well as the elastoplastic response of a fibrous composite, are provided.

3.2 MATHEMATICAL FORMULATION

The formulation comprises two parts. First, the elastoplastic behaviour of a medium consisting of two/three families of mutually orthogonal and equally spaced layers is modeled with the aid of the concept of a superimposed medium. An appropriate orientation average, corresponding to the given problem is subsequently established. With no loss of generality, only the formulation for a fibrous composite is presented and the extension to a particle reinforced composite can be readily accomplished with one more family of layers involved.

Consider an elastic medium with the elastic properties of reinforcement intercepted by two families of mutually orthogonal layers possessing the elastoplastic properties of the matrix. In order to describe the average mechanical properties of this system, it is convenient to address the influence of the two families of layers separately, i.e., invoke the concept of a superimposed medium.

Consider first the medium with equally spaced horizontal layers. Suppose that the mechanical properties of reinforcement and the layer material are identified by the following constitutive equations

$$\dot{\sigma}^{f} = [D^{f}]\dot{\epsilon}^{f} \tag{3.1}$$

$$\dot{\sigma}^{m(1)} = [D^{m(1)}]\dot{\epsilon}^{m(1)} \tag{3.2}$$

in which $[D^{f}]$ is the elastic stiffness of reinforcement, $[D^{m(1)}]$ is the elastoplastic stiffness of the material of the horizontal layers, and $\dot{\sigma}=\{\dot{\sigma}_{11},\dot{\sigma}_{22},\dot{\sigma}_{33},\dot{\sigma}_{12},\dot{\sigma}_{13},\dot{\sigma}_{23}\}^{T}$ and $\dot{\epsilon}=\{\dot{\epsilon}_{11},\dot{\epsilon}_{22},\dot{\epsilon}_{33},\dot{\gamma}_{12},\dot{\gamma}_{13},\dot{\gamma}_{23}\}^{T}$ are the stress and strain rates respectively, with the different superscripts indicating distinct constituents. Both constituents are assumed to exit simultaneously and to be perfectly bonded, so that the overall stress and strain rate averages $\dot{\sigma}^{(1)}$ and $\dot{\epsilon}^{(1)}$ can be derived from the averaging rule (Hill, 1963)

$$\dot{\epsilon}^{(1)} = \eta_{11}\dot{\epsilon}^{f}+\eta_{12}\dot{\epsilon}^{m(1)} \tag{3.3}$$

$$\dot{\sigma}^{(1)} = \eta_{11}\dot{\sigma}^{f}+\eta_{12}\dot{\sigma}^{m(1)} \tag{3.4}$$

where η's are the respective volume fractions of the constituents

$$\eta_{11} = \frac{h}{h+t} \quad ; \quad \eta_{12} = \frac{t}{h+t} \tag{3.5}$$

and h and t denote the spacing and the thickness of the layers, respectively.

The assumption of perfect bonding between the constituents and the equilibrium requirements provide additional kinematic and static constraints

$$[\delta_1]\dot{\sigma}^{f} = [\delta_1]\dot{\sigma}^{m(1)} \tag{3.6}$$

$$[\delta_1^*]\dot{\epsilon}^{f} = [\delta_1^*]\dot{\epsilon}^{m(1)} \tag{3.7}$$

where

$$[\delta_1] = \begin{bmatrix} 0 & 0 & 1 & 0 & 0 & 0 \\ 0 & 0 & 0 & 0 & 1 & 0 \\ 0 & 0 & 0 & 0 & 0 & 1 \end{bmatrix} \quad ; \quad [\delta_1^*] = \begin{bmatrix} 1 & 0 & 0 & 0 & 0 & 0 \\ 0 & 1 & 0 & 0 & 0 & 0 \\ 0 & 0 & 0 & 1 & 0 & 0 \end{bmatrix}$$

It is evident that the field equations listed above (eqs.(3.1)-(3.4)), together with eqs.(3.6) and (3.7), render a set of 30 equations for 30 unknowns, e.g. $\dot{\sigma}^{(1)}$, $\dot{\sigma}^{f}$, $\dot{\sigma}^{m(1)}$, $\dot{\epsilon}^{f}$ and $\dot{\epsilon}^{m(1)}$. Thus, the problem is mathematically determinate. The solution (Pietruszczak and Niu, 1991) takes the form

$$\begin{aligned} \dot{\sigma}^{(1)} &= [D^{(1)}]\dot{\epsilon}^{(1)} \\ [D^{(1)}] &= \eta_{11}[D^{f}][S_{11}]+\eta_{12}[D^{m(1)}][S_{12}] \end{aligned} \tag{3.8}$$

where $[S_{11}]$ and $[S_{12}]$ are known as strain concentration tensor

$$\dot{\epsilon}^{f} = [S_{11}]\dot{\epsilon}^{(1)} \quad ; \quad \dot{\epsilon}^{m(1)} = [S_{12}]\dot{\epsilon}^{(1)} \tag{3.9}$$

and are functions of both the mechanical properties of the constituents and the respective volume contributions. The details concerning the derivation of eq.(3.8) are provided in Section 3.6.

Assume now that the homogenized medium, whose response is defined by eq.(3.8), is intercepted by the second family of layers. In such a case, one has

$$\dot{\sigma}^{m(2)} = [D^{m(2)}]\dot{\epsilon}^{m(2)} \tag{3.10}$$

together with the set of equations analogous to eqs.(3.3) and (3.4), i.e.

$$\dot{\sigma} = \eta_{21}\dot{\sigma}^{(1)}+\eta_{22}\dot{\sigma}^{m(2)} \tag{3.11}$$

$$\dot{\epsilon} = \eta_{21}\dot{\epsilon}^{(1)}+\eta_{22}\dot{\epsilon}^{m(2)} \tag{3.12}$$

Here η's are the volume contributions of the constituents

$$\eta_{21} = \frac{h}{h+t} \quad ; \quad \eta_{22} = \frac{t}{h+t} \tag{3.13}$$

whereas h and t represent the spacing and the thickness of the second family of layers (not necessarily identical to those of the first family). The kinematic and static constraints can be specified as

$$[\delta_2]\dot{\sigma}^{(1)} = [\delta_2]\dot{\sigma}^{m(2)} \tag{3.14}$$

$$[\delta_2^*]\dot{\epsilon}^{(1)} = [\delta_2^*]\dot{\epsilon}^{m(2)} \tag{3.15}$$

where

$$[\delta_2] = \begin{bmatrix} 0 & 1 & 0 & 0 & 0 & 0 \\ 0 & 0 & 0 & 1 & 0 & 0 \\ 0 & 0 & 0 & 0 & 0 & 1 \end{bmatrix} \quad ; \quad [\delta_2^*] = \begin{bmatrix} 1 & 0 & 0 & 0 & 0 & 0 \\ 0 & 0 & 1 & 0 & 0 & 0 \\ 0 & 0 & 0 & 0 & 1 & 0 \end{bmatrix}$$

Following a similar procedure to that established for the first family of layers, one obtains

$$\begin{gathered} \dot{\sigma} = [D]\dot{\epsilon} \\ [D] = \eta_{21}[D^{(1)}][S_{21}]+\eta_{22}[D^{m(2)}][S_{22}] \end{gathered} \tag{3.16}$$

where $[S_{21}]$ and $[S_{22}]$ are the strain concentration tensors

$$\dot{e}^{(1)} = [S_{21}]\dot{e} \quad ; \quad \dot{e}^{m(2)} = [S_{22}]\dot{e} \tag{3.17}$$

Substitution of eq.(3.8) in eq.(3.16), results in

$$\begin{aligned}[D] = {} & \eta_{21}\eta_{11}[D^f][S_{11}][S_{21}]+ \\ & \eta_{21}\eta_{12}[D^{m(1)}][S_{12}][S_{21}]+\eta_{22}[D^{m(2)}][S_{22}]\end{aligned} \tag{3.18}$$

It is noted that the first term in eq.(3.18) represents the contribution of the reinforcement, whereas remaining terms refer to the matrix. In view of eqs.(3.17) and (3.9), the strain rates in the constituents can be related to their overall counterparts

$$\dot{e}^f = [S_{11}][S_{21}]\dot{e} \quad ; \quad \dot{e}^{m(1)} = [S_{12}][S_{21}]\dot{e} \tag{3.19}$$

Consider now a composite reinforced by long cylidrical fibres which are randomly dispersed in the transverse plane. The response of such a system is assumed to be defined by eq.(3.16) providing the orientation average in the transverse plane is taken

$$\dot{\sigma}' = [D']\dot{e}' \quad ; \quad [D'] = \frac{1}{\pi}\int_0^{\pi}[T'][D][T]d\beta \tag{3.20}$$

In eq.(3.20) $\dot{\sigma}'$ and $\dot{\epsilon}'$ represent the stress and strain rates of a fibrous composite, [D] is given by eq.(3.18), whereas [T′] and [T] represent the transformation matrixes defined as

$$a' = [T']a \quad ; \quad a = [T]a'$$

where a′ and a symbolize symmetric second order tensors expressed as vectors in a six-dimensional space. Both [T′] and [T] can be writen in the explicit form

$$[T'] = \begin{bmatrix} 1 & 0 & 0 & 0 & 0 & 0 \\ 0 & c^2 & s^2 & 0 & 0 & -2cs \\ 0 & s^2 & c^2 & 0 & 0 & 2cs \\ 0 & 0 & 0 & c & -s & 0 \\ 0 & 0 & 0 & s & c & 0 \\ 0 & cs & -cs & 0 & 0 & c^2-s^2 \end{bmatrix} \quad ; \quad [T] = \begin{bmatrix} 1 & 0 & 0 & 0 & 0 & 0 \\ 0 & c^2 & s^2 & 0 & 0 & 2cs \\ 0 & s^2 & c^2 & 0 & 0 & -2cs \\ 0 & 0 & 0 & c & s & 0 \\ 0 & 0 & 0 & -s & c & 0 \\ 0 & -cs & cs & 0 & 0 & c^2-s^2 \end{bmatrix}$$

in which $c=\cos\beta$ and $s=\sin\beta$.

For a particle reinforced composite one more family of layers, perpendicular to the former two, should be introduced and the orientation averaging scheme, eq.(3.20), should be replaced by a three-dimensional one. In what follows, the proposed approach is investigated in detail. First, the elastic properties of fibre and particle reinforced composite systems are determined and subsequently the elastoplastic response of a fibrous composite is studied.

3.3 ELASTIC PROPERTIES OF LONG FIBRE AND PARTICLE REINFORCED COMPOSITES

In general, the orientation average, eq.(3.20), has to be evaluated numerically since the form of the stiffness matrix [D] in eq.(3.20) is orientation dependent. If all constituents remain elastic, however, the integration can be carried out analytically. For the later case, eq.(3.20) yields

$$
\begin{gathered}
D'_{11} = D_{11}\ ; \quad D'_{22} = (3D_{22}+3D_{33}+2D_{23}+2D_{66})/8 \\
D'_{33} = D'_{22}\ ; \quad D'_{44} = (D_{44}+D_{55})/2 \\
D'_{55} = D'_{44}\ ; \quad D'_{66} = (D_{22}+D_{33}-2D_{23}+2D_{66})/2 \\
D'_{12} = D'_{13}\ ; \quad D'_{13} = (D_{12}+D_{13})/2 \\
D'_{23} = D'_{32}\ ; \quad D'_{23} = (D_{22}+D_{33}+6D_{23}-2D_{66})/8
\end{gathered}
\tag{3.21}
$$

It is noted that [D] corresponds to an orthotropic material, whereas [D′] is that of transversely isotropic one. In terms of elastic constants, one has (see Hashin and Rosen, 1964)

$$
\begin{gathered}
K_{23} = (D'_{22}+D'_{23})/2\ ; \quad G_{23} = (D'_{22}-D'_{23})/2 \\
G_{12} = D'_{44}\ ; \quad E_{11} = D'_{11}-2D'^{2}_{12}/(D'_{23}+D'_{22}) \\
\nu_{12} = \frac{1}{2}(D'_{11}-E_{11})^{1/2}/K_{23}
\end{gathered}
$$

Numerical simulations have been performed for glass fibres and epoxy matrix. The elastic constants of both constituents have been assumed after Zhao and Weng (1990)

Fibres: $E_f=72.4$ GPa, $\nu_f=0.20$

Matrix: $E_m=2.76$ GPa, $\nu_m=0.35$

Fig.3.1 presents the variation of the five elastic constants as predicted by eq.(3.21). The results have been compared with those obtained from the equivalent inclusion method (Zhao and Weng, 1990), which is based on Eshelby's solution of ellipsoidal inclusion (Eshelby, 1957) and Mori-Tanaka mean field theory (Mori and Tanaka, 1973). It can be seen that the estimates based on the two approaches are very close.

For a composite reinforced with randomly distributed particles, an appropriate three-dimensional orientation average has to be evaluated. In such a case, transformation matrices [T′] and [T] in eq.(3.20) are function of three independent variables, for instance Euler angles. It is obvious that lengthy algebraic manipulations are unavoidable in order to arrive at an analytical solution. An alternative is to establish the orientation average specified in eq.(3.20) first, and introduce a spherical coordinate system in order to perform the subsequent averaging. The latter approach was suggested by Christensen and Waals (1972) and results in

$$D_{33} = (3D'_{11}+8D'_{22}+4D'_{12}+4D'_{44})/15$$

$$D_{23} = (D'_{11}+D'_{22}+8D'_{12}+5D'_{23}-2D'_{44})/15$$

where [D′], eq.(3.20), is established by inserting one more family of layers to create a laminate system strengthened by cubic particles. The bulk and shear moduli are defined as

$$K = (D_{33}+D_{23})/2 \quad ; \quad G = (D_{33}-D_{23})/2$$

The numerical simulations have been performed using the same elastic constants as those for the fibrous composite and the results are presented in Fig.3.2. Again, a good agreement with the solution based the equivalent inclusion method (Weng, 1973) can be observed.

3.4 ELASTOPLASTIC RESPONSE OF FIBROUS COMPOSITE

In this section, the elastoplastic behaviour of boron/aluminum composite system is investigated. The mechanical properties of this composite are taken from the literature (Kenaga, Doyle and Sun, 1987; Sun and Chen, 1991). The elastic constants and the volume fractions are as follows

Boron fibres: $E_f=379.3$ GPa, $\nu_f=0.1$

Aluminum matrix: $E_m=68.3$ GPa, $\nu_m=0.3$

Volume fractions: $c_f=0.47$, $c_m=0.53$

The matrix is assumed to be a von Mises material with isotropic hardening obeying an associated flow rule. The yield function is given by

$$f = \bar{\sigma} - \kappa(\xi) \quad ; \quad \bar{\sigma} = \sqrt{\frac{3}{2} S_{ij} S_{ij}}$$

in which S_{ij} represents deviatoric stress tensor and the hardening function $\kappa(\xi)$ is selected in the hyperbolic form

$$\kappa(\xi) = \sigma_s + (\sigma_f - \sigma_s)\frac{\xi}{\xi + A}$$

where σ_s and σ_f denote the initial tensile yield stress and ultimate stress respectively, and A is a material constant. The hardening parameter is defined as

$$\xi = \int \sqrt{\frac{2}{3} de_{ij}^p de_{ij}^p}$$

in which de^p_{ij} represents the deviatoric plastic strain rate. From the information provided in papers by Kenaga, et al. (1987) and Sun and Chen (1991), it can be estimated that σ_s=43 MPa, σ_f=76 MPa and A=0.00276. The tensile stress-strain diagram is re-plotted in Fig.3.3. Following the standard plasticity procedure, the elastoplastic stiffness matrix can be established.

In order to evaluate the orientation average, eq.(3.20), Gaussian quadrature has been employed. Five Gaussian sample points were chosen within the interval [0, π]. The averaging scheme has been tested first in the context of elasticity, yielding the results identical to those obtained from the analytical solution, eq.(3.21). The scheme has been subsequently tested for elastoplastic response. The stress-strain response of transverse uniaxial tensions and longitudinal pure shears is shown in Fig.3.4. It can be seen that the inherent isotropy of a fibrous composite has been preserved and consequently the averaging scheme is acceptable.

Fig.3.5 shows the uniaxial tensile stress-strain curves, in which ϑ indicates the orientation of fibres with respect to the direction of tensile stress. It can be seen that the predicted response is generally stiffer than the experimental one. For $\vartheta \leq 45°$, reasonable results are obtained, however the curve for $\vartheta = 60°$ lies above that for $\vartheta = 45°$. The latter result is consistent with the assumption of perfect bonding and indicates however that for large values of ϑ other mechanisms, such as slippage and separation between fibres and matrix, contribute to the elastoplastic stress-strain response. Fig.3.6 depicts the variation of the tensile strength with the orientation of fibres. It can be seen that for $\vartheta = 45°$ the tensile strength reaches the minimum value. The maximum value of 2004 MPa corresponds to $\vartheta = 0°$. Furthermore, it can be observed that the tensile strength is highly overestimated for large values of ϑ.

3.5 CONCLUSIONS

A micro-mechanical approach has been suggested for modelling the elastoplastic behaviour of perfectly bonded composite systems. The approach has been based on the concept of a superimposed medium combined with appropriate orientation averaging schemes. The overall mechanical properties of a medium embodying two/three families of mutually orthogonal layers have been established by considering their influence separately. In conceptual terms, such a procedure results in creating a laminate system strengthened by square fibres or cubic particles. Such a system is supposed to approximate the response of a fibre/particle reinforced composite system after the orientation average is taken.

The elastic response of fibre/particle reinforced composites has been simulated. The proposed approach furnishes very reasonable predictions in comparison to the solutions from the equivalent inclusion method. The elastoplastic analysis results in quite reasonable estimates which are consistent with the assumption of perfect bonding. A more precise microscopic description of the elastoplastic behaviour requires the incorporation of other mechanisms such as slippage and separation at the interfaces between constituents.

3.6 APPENDIX:DERIVATION OF STRAIN CONCENTRATION TENSORS

In order to provide an explicit form of the overall constitutive relation, it is convenient to introduce the following identities